

SUPPORTING REPORT[L]

GEOMORPHOLOGY, GEOLOGY AND GROUNDWATER

ANNEX L: GEOMORPHOLOGY, GEOLOGY AND GROUNDWATER
CONTENTS

L.	GEOMORPHOLOGY,GEOLOGY,AND GROUNDWATER	
L.1	Geomorphology	L-1
L.2	Geology	L-2
L.3	Groundwater	L-4
L.4	Water Quality	L-8
L.5	Results of Resistivity Sounding	L-8

L. Geomorphology, Geology, and Groundwater

L.1 Geomorphology

The Jiboa River Basin is divided into a mountainous/hilly area in the northern area and a flat plain in the southern downstream area. The two areas are approximately separated by the contour line of 100 m in elevation.

Figure L.1 shows a topographic map contoured using 1 km x 1 km nodal elevations read from 1:50,000 scale topographic maps. Then the contour lines are drawn by interpolating every 500 m the nodal elevation by the Kriging method. Therefore, the map can be treated as a summit surface map because the map neglects minor ridges and valleys.

From the map, the upstream area in the basin can be subdivided into the outer ring mountains surrounding Ilopango caldera, the foothill area of the southern outer ring mountains, the foot of San Vicente Volcano, and the hilly areas on the left side of El Desague river and the upstream area of the Jiboa river.

Figure L.2 shows three-dimensional topographic images made from the above interpolated data. The geomorphologic features obtained from Figures L.1 and L.2 can be summarized as follows:

- 1) The scale of erosion along Jiboa river is the biggest from the view point of geomorphology. The second may be the area along which the Comalapa river flows down to the west of the study area. The erosional scale of Rio Sepaquiapa is bigger than that of Rio Tilapa.
- 2) A clear topographic boundary line can be recognized from El Desague river to the east through Jiboa river. This coincides with the geological tectonic line indicated in the Geological maps of the Republic of El Salvador (1978). It is presumed that the area south of the tectonic line might have been downthrown.
- 3) A gentle slope at elevations between 600 to 700 m can be seen in the areas of Candelaria, San Ramon, and San Cristobal in the upper basin based on the 1 km interval elevation data. This indicates that the scale of present erosive topography is less than 1 km in size and the primitive topography of the area before erosion was almost flat.

In general, it is understood that the distribution of groundwater levels show a good agreement with the rough topography. In the study area, as described in a later chapter, the depths to groundwater from the ground surface are deeper on the ridges in the mountainous/hilly areas and the slope of groundwater table becomes gentle compared with the topographic slope in higher elevation areas. However, it is predicted that the elevations of groundwater table in the study area are generally the same as the river bed elevations.

In addition, aerial photo interpretation was carried out in the downstream area. The terraces elevated 1 to 2 m from Jiboa river are found both sides of the river. The old river courses are also clearly found from the aerial photo interpretation.

L.2 Geology

1) Stratigraphy

The study area is underlain by mainly volcanic sediments of Tertiary to Quaternary age. According to references such as "Mapa Geologico de la Republica de El Salvador" (1978), the geology of the study area consists of BALSAMO Formation (Miocene to Pliocene), CUSCATLAN Formation (Pliocene to Pleistocene), and SAN SALVADOR Formation (Pleistocene to Holocene) in ascending order.

The features and distribution of each formation and geologic structures are as follows:

a) Balsamo Formation

The Balsamo Formation mainly consists of basaltic volcanic sediments and ejecta. Pyroclastic flow sediments are distributed in areas of the upper portion of Ilopango outer ring mountains, San Pedro Masahuat, Rosario to midstream of the Jiboa river, and the western foot of San Vicente Volcano.

Basaltic lava and tuff breccia occur at the areas along top of the Ilopango outer ring mountains, San Juan Tepezontes to San Emigdio, Cojutepeque, some areas from San Ramon to San Cristobal, and Guadalupe to San Pedro Nonualco on the western foot of San Vicente Volcano. The basaltic lava is usually underlain by tuff breccia, which color to be has been changed to reddish brown to dark brown.

Hydrogeologically the lava layers having fissures and cracks could be good aquifers, however, other facies may have small values of hydraulic conductivity because the sediments are well consolidated.

b) Cuscatlan Formation

The Cuscatlan Formation is mainly composed of acidic pyroclastics and volcanic sediments, unconformably overlying the Balsamo Formation. The massive well consolidated ignimbrite can be observed at the areas along the highway between San Salvador and the international airport and in the hill slopes around Tapalhuaca, San Pedro Masahuat, and Rosario. On the other hand, relatively consolidated pumice tuff is widely distributed around the San Ramon to San Cristobal areas in the upper basin and the area west of midstream Jiboa river. At some parts in the upstream area, lahar deposits and lake sediments occur.

Groundwater occurs in fissures and cracks in the ignimbrite because the rock has low permeability and is massive in nature. The hydraulic conductivity of pumice tuff in the upper basin varies depending on its facies; the fine tuff has relatively small hydraulic conductivity.

c) San Salvador Formation

In and around the study area, any formations from late Pleistocene to Holocene are called the San Salvador Formation. The San Salvador Formation consists of many different facies such as acidic pyroclastic sediments, Holocene volcanic ejecta, fluvial and alluvial deposits in the downstream area, etc. The Holocene pumiceous pyroclastic sediments are distributed widely on the flat plains and gentle slopes in the study area. The pyroclastic sediments are not consolidated resulting in many land failures and considerable erosion in these areas.

According to the well data in the downstream area, the subsurface geology in the area consists of sand, gravel, and clayey sediments of Pleistocene to Holocene. On the terrace, Holocene pumice tuff covers the fluvial sediments.

2) Geologic structures

The geologic structures in the study area are characterized by Ilopango caldera, E-W fault zone located along the northern foot of San Vicente Volcano, NE-SW fault system along the midstream Jiboa river, and NW-SE fault systems in the middle to upper basin.

a) Ilopango caldera

Ilopango is a caldera that said to be formed in 260 AD. Ash from this explosive eruption covered much of central El Salvador. Lake Ilopango fills part of the caldera. Islas Quemadas, a volcanic dome, formed within the caldera in 1879-1880.

The average lake water level of Ilopango is 440.30 m in elevation; the water level ranges from 439.45 m to 441.15 m. The depth to the water exceeds 200m in the central part of the lake. The island of Quemadas stands from the lake bottom at depths from 220 m to 230 m.

b) E-W fault zone located along the northern foot of San Vicente Volcano

The fault traces from the eastern part of Ilopango lake to San Vicente city along the El Desague river, and divides the area into the hilly area to the north and the foot of San Vicente Volcano to the south. To the north of Verapaz, difference of elevation along the fault is about 150 m. The elevation difference becomes larger to the east. There are several natural spring sites along the fault, indicating that the groundwater flow system in the area is controlled by the fault.

c) NE-SW fault system along the midstream Jiboa river

The geologic map shows the existence of a fault extending from the intersection of El Desague and the Jiboa rivers to the intersection of the Jiboa and Chinuapa rivers. This fault can be traced to the northeast up to the area around San Sebastian, being displaced by the E-W fault mentioned above.

d) NW-SE fault systems in the middle to upper basin

The geologic maps show many faults and estimated faults in the areas from Cojutepeque to San Pedro Masahuat. Meanwhile a NNW-SSE fault system can be seen in the areas of San Antonio Masahuat, San Pedro Masahuat, and Tapalhuaca. As expected, the many faults strongly influence and control the surface drainage patterns and groundwater. The rocks and sediments in these areas are well fractured as a result of the high density of faults.

L.3 Groundwater

The resistivity sounding and data collection/interpretation of existing wells were carried out to better understand subsurface geologic structures and the groundwater system.

1) Resistivity sounding

Resistivity soundings using the Wenner electrode array was carried out at 31 locations in and around the study area. The sounding locations are shown in Figure L.3. The maximum distance between the outer electrodes extended to 396 m. The apparent resistivity values were read 31 times at fixed electrode intervals shown in the data sheets attached in the Annex. The theoretical depth of investigation of the resistivity sounding is 132 m ($396 \text{ m} / 3 = 132 \text{ m}$).

Table L.1 shows the list of resistivity soundings with the apparent resistivity curve types.

There are two methods of interpretation; one is the traditional graphical method using two layer standard curves with supplemental curves, and the other is the method using inversion techniques. In this study, the traditional method was employed in the field to obtain the initial values for the inversion model, then the values were input to the inversion interpretation program called "RINVERT".

Table L.2 summarizes the results of the inversion analysis (top and bottom elevations of each resistivity layer and the resistivity). All data sheets and apparent resistivity curves with results of inversion model analysis are presented in the Annex.

It is necessary to examine the correlation between the resistivity layer classification and actual subsurface geologic information obtained from boring cores and/or well logs for estimating subsurface geology from the results of resistivity soundings. Figure L.4 shows the correlation of resistivity sounding results with the existing lithologic logs at site E-01, San Ramon. The figure indicates that the resistivity value changes at the weathered zone in the andesite lava layer at a depth of about 20 m.

Generally the resistivity values of coarse materials are higher and the values of fine sediments such as clay and silt are lower. The lava in volcanic regions usually are a higher resistivity value. In addition, even in the same volcanic region, the resistivity values increase with increasing the elevation because there are more coarse materials near the top of a volcano.

For hydrogeological purposes, the interpretation results of resistivity soundings are used to find the

occurrence of possible aquifers. For instance, a high resistivity layer in coastal areas may indicate a gravel layer, which could be a good aquifer in the areas. In volcanic areas, a high resistivity layer may indicate a lava layer, that could yield a good amount of groundwater. It is noted that the resistivity values vary within a geologic layer if the groundwater table is located in the layer. In other words, the resistivity value in an unsaturated zone is different from that in a saturated zone. Therefore, groundwater levels at nearby wells were measured during the field work. It should also be noted that if the groundwater quality is saline, the resistivity values become small and it is difficult to identify any aquifers from the resistivity survey.

Analysis and interpretation of resistivity data show that K and Q type curves are common in the downstream area (E-07, 08, 11, 12, 21, 22, 23), indicating that resistivity values decrease with depth. In this coastal plain area, the geology consists primarily of recent fluvial sediments which are unconsolidated to moderately consolidated. Typically the resistivity value decreases by a magnitude of order within the first few meters. This generally corresponds with the river water levels and the shallow groundwater levels measured in nearby shallow wells. Resistivity values continue to decrease which indicates sediments are finer grained and/or more compacted. In many of the resistivity sounding records a thin zone of very low resistivity is encountered. This is probably a layer of clay or volcanic ash and in some areas will separate groundwater zones or create perched water tables of limited capacity.

Also, near the coast (E-23) the resistivity value is very low and becomes lower. This relationship is typically associated with the presence of saline water. It is quite likely that there is a salt-water zone extending inland a short distance from the ocean. However, the extent of such a zone is difficult to verify without additional data.

To the north, in the area near San Pedro Masahuat and San Antonio Masahuat (E-02, 18), there is a thin zone of sharply higher resistivity. Considering the geology of the area and proximity to Ilopango caldera, this is interpreted to be a thin lava layer or similar volcanic deposits.

In the upstream areas, the resistivity data is commonly represented by A and H type curves (E-09,10, 15, 24, 25, 27), indicating that resistivity increases with depth. This relationship is a result of the widespread distribution of andesitic and basaltic lavas underlying the sediments in this area. Typically, lava flows have a weathered surface, which is clayey, and are overlain by consolidated sediments of the Cuscatlan Formation. Usually there is a shallow water table perched on the weathered surface, which is not very productive but yields water in the wet seasons. The deeper water table in the confined aquifer is a better source for water generally, but difficult to access due to the depth. Also, since many wells are constructed without the aid of modern drilling machinery, hard rocks are relatively impermeable for well construction using manual methods.

2) Collection and interpretation of existing well data

The study team collected 54 well data in and around the study area. These are tabulated as shown in Table L.3. Most of these wells were drilled by ANDA and PLANSAVAR. The location of existing wells are

shown in Figure L.5. The existing wells are distributed in the downstream area and the northern area from Ilopango lake. However, there are also a few wells in the upstream area of Jiboa river, but no well data are available in the midstream hilly area.

Although the distribution of well data is not uniform in the study area, a specific capacity map is prepared to understand the aquifer characteristics in the study area (Figure L.6). The values of specific capacity can easily be obtained from pumping tests or well production test as follows:

$$(\text{Specific capacity}) = (\text{Discharge rate}) / (\text{Drawdown})$$

It can be said that the aquifer productivity increases with increasing specific capacity. According to Figure L.6, the areas having more than 500 m²/day in specific capacity can be seen in near Rosario, the northern part of Ilopango lake, and the foot of San Vicente Volcano. There is no well data in the upstream area of San Pedro Masahuat and San Antonio Masahuat, however, it is estimated that the areas may have 250 to 500 m²/day in specific capacity based on the results of resistivity sounding and the geologic conditions.

On the other hand, the area having less than 100 m²/day in specific capacity is found from the northwestern part of the international airport to the west side bank of Jiboa river, indicating that the aquifer productivity in the area is relatively poor. The aquifer productivity at the coastal area is medium because the specific capacity ranges from 100 to 200 m²/day.

The areas of San Ramon and Santo Domingo have relatively small specific capacity ranging from 50 to 100 m²/day.

Figure L.7 shows the relationship between transmissivity obtained from pumping tests at existing wells and specific capacity, in which the existing wells are classified into three areas; viz. the upstream area, Rosario area in midstream, and the downstream area. The relation between transmissivity (T) and specific capacity (Sc) in the upstream area can be expressed as:

$$T = 1.234 Sc$$

In Rosario area, both T and Sc are higher than those in other areas, the relation is:

$$T = 1.165 Sc$$

And the relation in the downstream area is obtained as:

$$T = 1.189 Sc$$

The following empirical equation presented by Logan (1964) is well known to express the relation

between transmissivity and specific capacity.

$$T = 1.22 Sc$$

Comparing the T - Sc relations in the study area with the Logan's empirical equation, average relation in the three areas are almost same as the Logan's equation.

As a result of the above mentioned investigation and analysis, the aquifer productivity in the Jiboa river basin can be summarized as follows:

- 1) Relatively high productivity area ($500 \text{ m}^2/\text{day} \leq Sc$): Rosario area, northern area of Ilopango lake, and foot of San Vicente Volcano
- 2) Moderately productive area ($100 \text{ m}^2/\text{day} \leq Sc < 500 \text{ m}^2/\text{day}$): hilly area in the mid-Jiboa basin and coastal area in downstream
- 3) Relatively poor productive area ($Sc < 100 \text{ m}^2/\text{day}$): Right side area of upper Jiboa river, near international airport in downstream

The results of groundwater level measurements by the existing wells and by our field surveys show that the depths to groundwater level from ground surface in the downstream area mostly range from 2 to 5 m. However, the depths to groundwater on the hills in midstream and upstream areas show 20 to 30 m. Figure L.8 shows the distribution of groundwater levels in the study area.

The groundwater in the upstream to midstream areas occurs as perched water and unconfined water, whereas the groundwater in the downstream area occurs as unconfined water and confined water. For example, some spring water besides the road in San Cristobal area yields from pumice tuff, which is originated from the perched water formed within the tuff layer. At the western area of Rosario, there are two aquifer systems; one is shallow unconfined aquifer having shallow groundwater levels about 2 to 3 m from ground surface, the other is deep confined aquifer having more than 20 m in depth to piezometric head.

3) Recommendations

Through the course of data collection and analyses several deficiencies and problems were encountered and observed. These are listed and discussed below.

a) Lack of data and incompleteness of existing records

During the course of data collection, particularly well records and logs, it was discovered that the records are kept at many different agencies. In some cases the records were organized and easy to access. But in most cases the records were difficult to find, unorganized, and incomplete. Previous reports were also difficult to find and verify. It is suggested that one government agency be responsible for the collection

and archival of previous records. This agency would also be responsible for issuing well construction permits and ensuring a minimum set of data are recorded for new wells.

b) Absence of time series or long term data for analysis

No record of long term measurements was found during the course of this study. In order to plan for future development of water resources, a consistent record of time series data, such as water levels and water quality, should be utilized to evaluate long term trends and the impact of development. A simple network of carefully selected well and stream sites to be measured at regular intervals would be sufficient to initiate a long term data record. By properly documenting the location, reference point, and details of the method and type of measurement, personnel can easily duplicate the measurements at regular time intervals such as weekly or monthly. With additional resources it may be possible to install recording devices at selected sites to automate part of the data collection.

c) Acute need for remediation and development of water resources

Many problems of water quality and supply were observed throughout the study area. Access to sufficient quantities of potable water are essential to the health all people. It was clear that many areas do not have sufficient quantities of water which is easily accessible and many people are forced to use water from the rivers and streams as a result. The rivers and streams, which are used for disposal of sewage, garbage, and industrial effluent, are highly polluted and not safe for consumption. A comprehensive plan should be designed and implemented. Part of the plan would prioritize the need for water in the various towns and villages, then provide detailed hydrogeologic investigations, followed by well and pump installation or spring development. Another part of the plan would be to establish a proper disposal system and clean up the rivers and streams. Attention to water supply and quantity will improve the health and longevity of the people.

L.4 WATER QUALITY

1) Groundwater

Figure L.9 shows that the distribution of major ions in the groundwater samples is clustered and generally within the expected range for groundwater. Samples taken during October 1996 have higher concentrations of carbonate ion (CO_3), approaching 100%. The major ion distribution does not vary significantly during the year.

Concentrations of Arsenic (As) and Boron (B) are quite high in samples taken from wells. In most of the wells sampled, As concentrations exceeded the WHO guidelines for drinking water and in 3 cases exceeded the FAO guidelines for agricultural irrigation water. Concentrations of B also exceeded the WHO guidelines for drinking water in 3 cases and the FAO guidelines in 1 case.

High concentrations of As are relatively common in areas with rocks and soils of volcanic origin. High concentrations of B are commonly associated with those of As, however, the source and mechanism are unclear.

2) Rivers

Water quality of rivers was analyzed 4 times during 1996. Figure L.10 shows the distribution of major ions for samples taken during October of 1996. Generally, the data are clustered near the middle of the diagram. These are slightly higher than expected concentrations of the ions. Sites R-1, 3, 4, 8, 9, and 10 are clustered near the 60% level for SO_4+Cl and the others are scattered around the 50% level for $Ca+Mg$. One exception is R-7, which has higher levels (70%, 50%) of both ion groups. These data trends are no doubt influenced by the various industrial and domestic pollutants discharged to the rivers.

As and B concentrations were quite high in the samples taken in February. Upon presentation of the data results from October samples, we will be able to establish any trends between the wet and dry seasons.

3) Hopango Lake

The results of the major ion analyses for samples taken in October 1996 are shown in Figure L.11. As expected in a large homogeneous body of water, the data are clustered very closely and don't change significantly during the course of the year. This is a good indicator that there is constant circulation in the lake and that stratification is not significant. The concentration SO_4+Cl is relatively high at 70-80%. Also, the concentration of $Na+K$ is quite high at 80%.

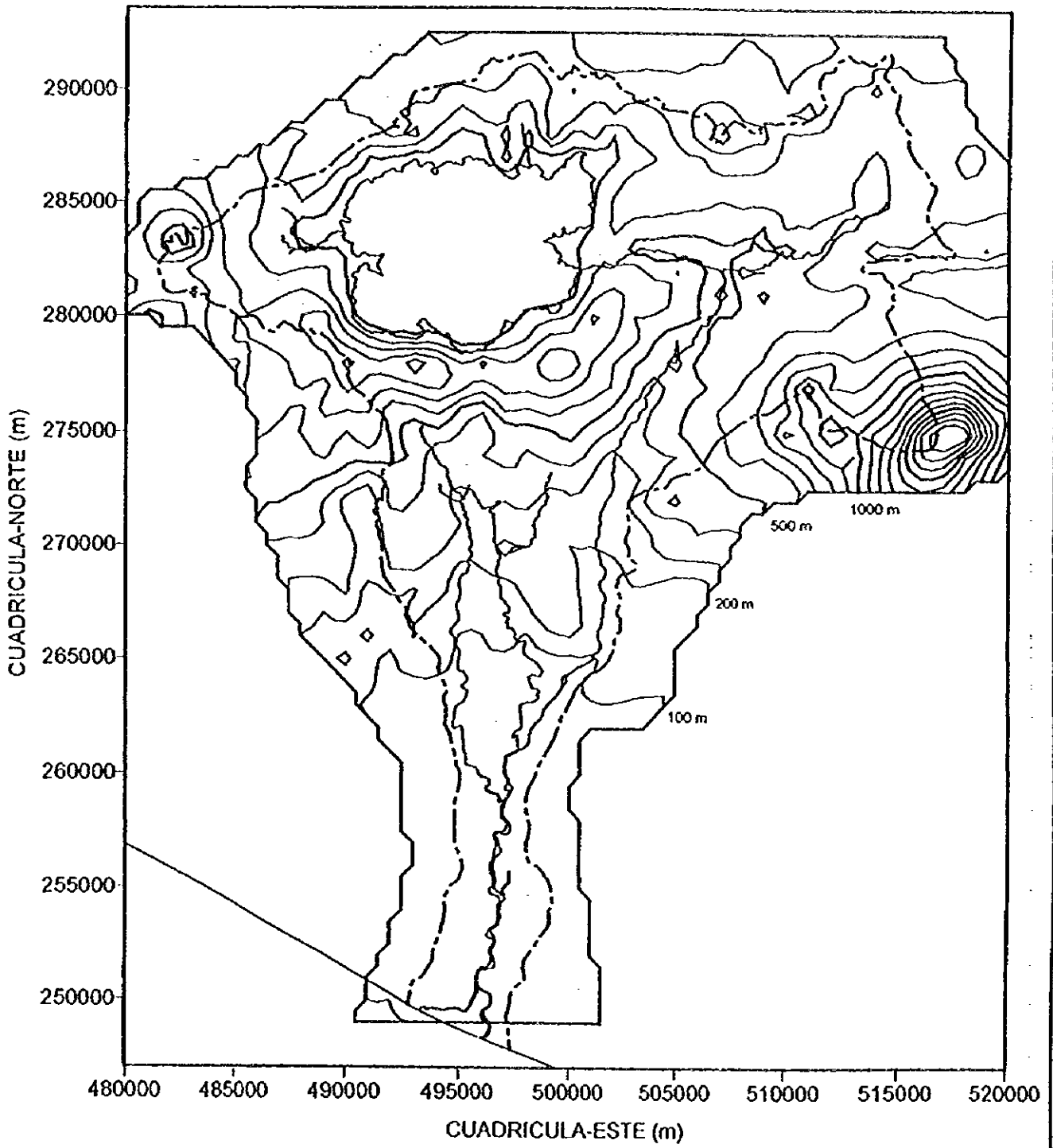
As and B concentrations were high in the February samples and most likely are at similar concentrations during the October sampling period. More details will be provided after the results of the data analysis are obtained.

4) Relations and interactions between groundwater and surface water

Figures L.12 and 13 show Stiff diagrams of the water quality data obtained during February and October of 1996. These diagrams show major ion concentrations for all sampled sites. It can be seen that during February, which is generally the dry season, the concentrations of ions in lake water cannot be traced downstream. This is because most of the rivers and streams are in baseflow or lowflow conditions, deriving water largely from groundwater. However, the results of the October sampling show a distinct trend and influence from Hopango lake water. The same Stiff pattern (high Na) can be seen in El Desague river and further downstream in the Jiboa river. This is due to higher runoff from the lake during the wet season. Further downstream concentrations of major ions increase starting from El Rosario. This is also due in part to increased runoff associated with the wet season.

Trends and patterns with As and B concentrations will be described after the results from the samples have been obtained.

During the dry season, baseflow conditions exist and groundwater influences the water quality of the rivers and streams. Ilopango lake water has an insignificant influence. During the wet season, Ilopango lake water is seen to have a strong influence on the major ion concentrations and distributions in the rivers and streams. At the same time, concentrations in groundwater decrease, probably due the infiltration of and dilution from precipitation.

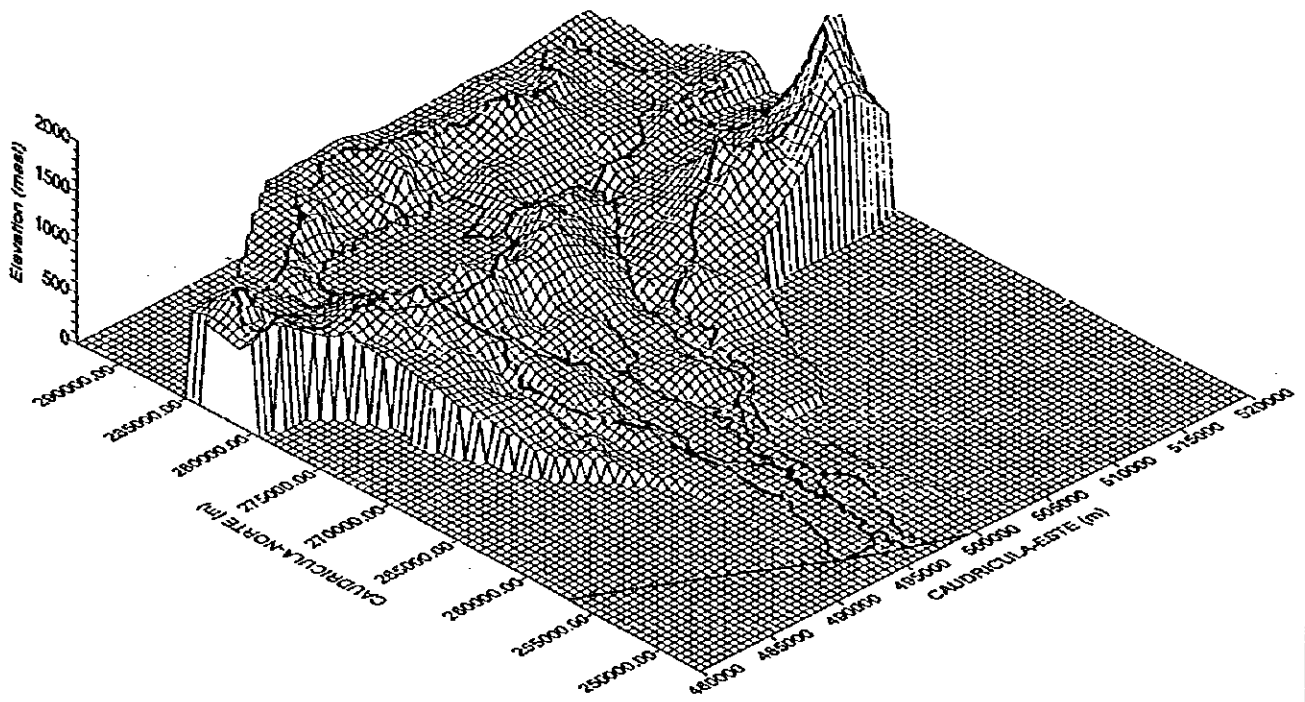


Counter line interval : 100 m

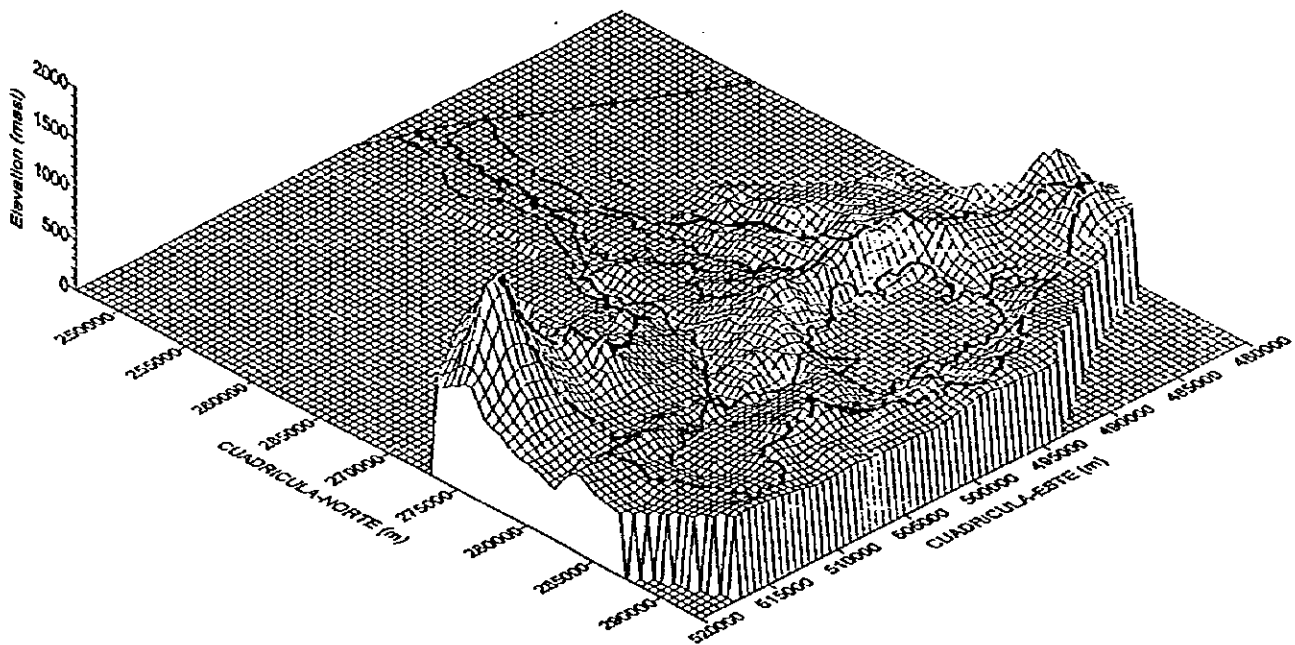
Thick counter line interval : 500 m

Counter lines are drawn by the Krining's interpolation methos.

FIG.1	TOPOGRAPHIC COUNTER MAP BASED ON 1km GRID NODAL DATA
AGENCIA DE COOPERACION INTERNACIONAL DEL JAPON (JICA)	



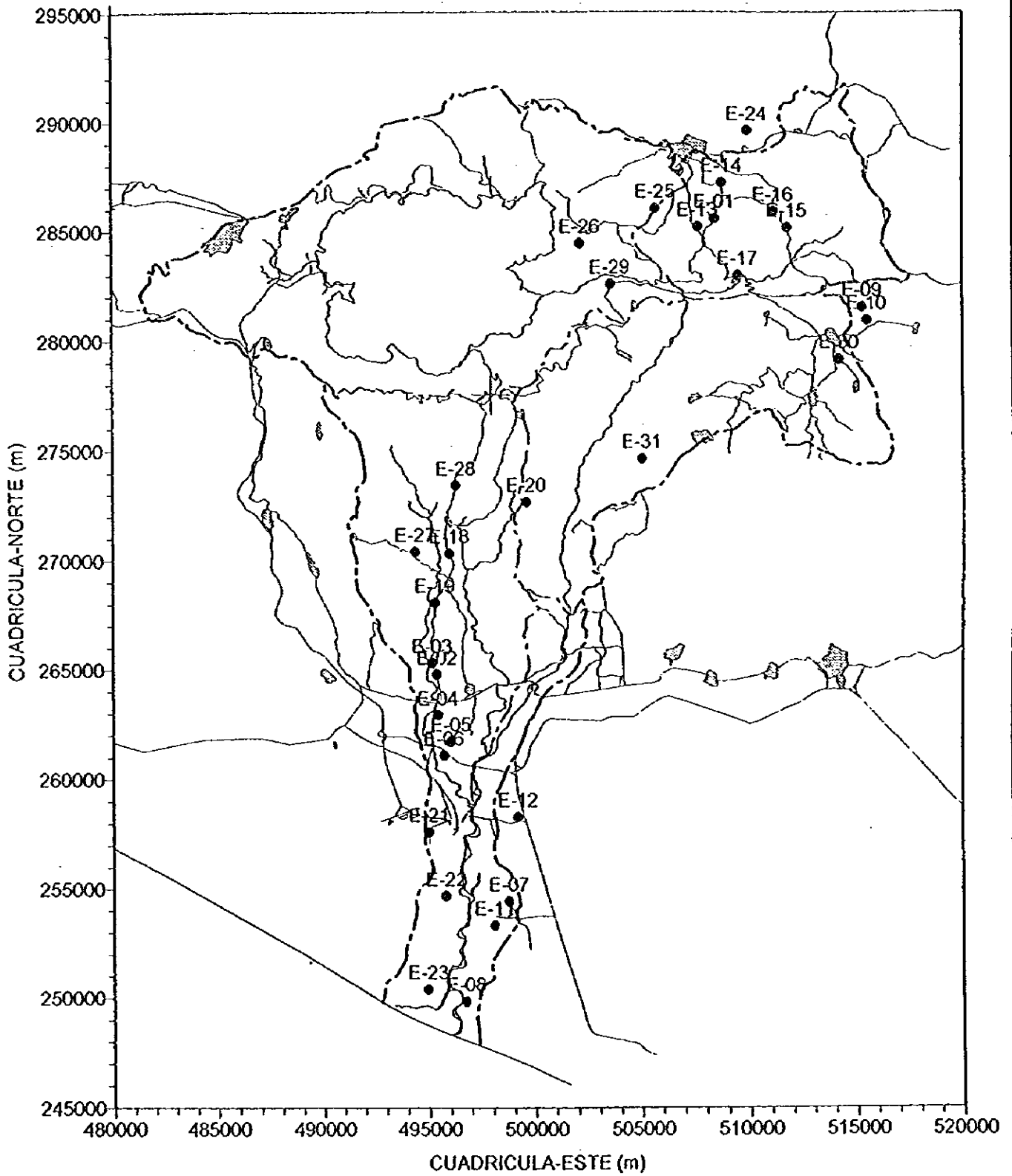
a) SW View



b) NE View

500 m nodal values are computed using the Kringing's interpolation method based on 1km x 1 km elevation data.

FIG. 2	3-D ORTHOGRAPHIC VIEW OF THE STUDY AREA
AGENCIA DE COOPERACION INTERNACIONAL DEL JAPON (JICA)	



E-01
 ● Location of resistivity sounding with No.

FIG.3	LOCATION OF RESISTIVITY SOUNDING
AGENCIA DE COOPERACION INTERNACIONAL DEL JAPON (JICA)	

Table 4.1.1 LIST OF RESISTIVITY SOUNDING

No.	E (m)	N (m)	Elev (m)	Curve type	Location
E-01	508412.5	285575	633	H	Cton. San Pablo, San Ramon
E-02	495350	264812.5	82	K	Cton. El Carmen, San Pedro Masahuat
E-03	495137.5	265350	88	Q	Cton. El Carmen, San Pedro Masahuat
E-04	495400	262962.5	69	HQ	Hda. Las Flores, San Pedro Masahuat
E-05	496000	261750	56	Q	Hda. San Mauricio, San Pedro Masahuat
E-06	495675	261125	46	QQ	Cton. Las Flores, San Pedro Masahuat
E-07	498725	254450	21	Q	Cton. Las Isletas, San Pedro Masahuat
E-08	496700	249875	6	Q	Hda. La Zorra, San Pedro Masahuat
E-09	515300	281550	602	HQ	Benef. Molineros, Tepetitán
E-10	515520	280950	610	H	Benef. Molineros, Tepetitán
E-11	498050	253362.5	17	Q	Hda. Santa Emilia, San Pedro Masahuat
E-12	499150	258325	34	Q	Desvio Las Tres Puertas, San Pedro Masahuat
E-13	507650	285200	633	A	San Ramon
E-14	508737.5	287250	775	K	Cton. San Pablo, San Ramon
E-15	511762.5	285175	635	KA	Cton. San Antonio, San Cristobal
E-16	511125	285912.5	641	KA	Cton. Santa Cruz, San Cristobal
E-17	509475	282975	495	K	Cton. Santa Anita, San Cristobal
E-18	495962.5	270350	232	K	Finca El Cocal, San Pedro Masahuat
E-19	495287.5	268100	170	Q	Barrio San Jose, San Pedro Masahuat
E-20	499600	272700	287	HQ	Cton. Belen, San Antonio Masahuat
E-21	494975	257625	24	HQ	Camp. El Cacao, San Pedro Masahuat
E-22	495763	254700	16	K	Camp. San Jose Luna, San Pedro Masahuat
E-23	494925	250425	5	K	Cton. Las Hojas, San Pedro Masahuat
E-24	509912.5	289650	772	H	Cton. Concepcion, El Carmen
E-25	505687.5	286075	667	K	El Llano, Candelaria
E-26	502125	284487.5	645	K	Cton. El Rosario, Candelaria
E-27	494375	270425	352	A	Cton. Buena Vista, Tapahuaca
E-28	496275	273462.5	381	A	Cton. El Socorro, San Antonio Masahuat
E-29	503537.5	282612.5	520	K	El Planon, Santa Cruz Analquito
E-30	514190	279150	672	K	Cton. San Antonio Los Ranchos, Guadalupe
E-31	505050	274662.5	505	KA	Cton. La Comunidad, San Pedro Nonualco

Curve Type:

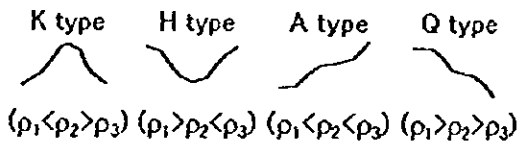


Table 4.1.2 LIST OF RESISTIVITY SOUNDING

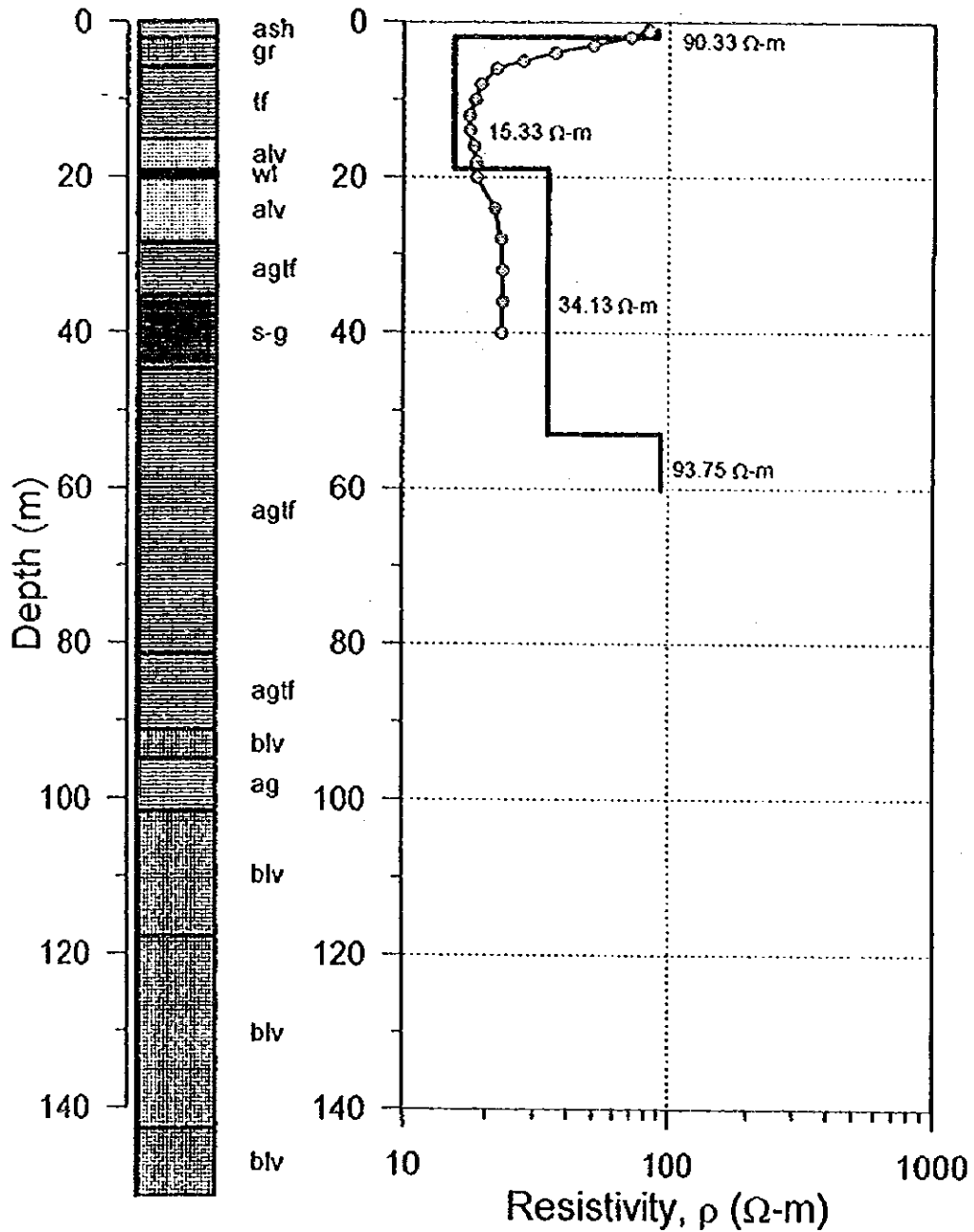
Sounding No.	Coordinates		Ground Elev. (m)	Layer-1		Layer-2		Layer-3		Layer-4		Layer-5		Layer-6		Layer-7	
	E (m)	N (m)		from(m)	to(m)	$\rho(\Omega\text{-m})$	from(m)	to(m)	$\rho(\Omega\text{-m})$	from(m)	to(m)	$\rho(\Omega\text{-m})$	from(m)	to(m)	$\rho(\Omega\text{-m})$	from(m)	to(m)
E-01	508412.5	285375	633	1.96	18.86	52.96	34.13	52.96	INFINITY	93.75	52.96	INFINITY	93.75				
E-02	495350	264812.5	82	2.2	3.29	155.99	35.34	155.99	INFINITY	Low	155.99	INFINITY	Low				
E-03	495337.5	265350	88	4.27	6.8	29.77	55.47	29.77	55.47	76.05	INFINITY	76.05	INFINITY	Low			
E-04	495400	262962.5	69	1.94	10.97	39.46	14.14	39.46	85.95	75.85	85.95	INFINITY	85.95	INFINITY	Low		
E-05	496000	261750	56	1.8	20.94	183.9	4.71	24.37	67.79	108.3	67.79	74.46	22.07	74.46	78.13	INFINITY	Low
E-06	495575	261125	46	2.98	38.64	41.98	Low	41.98	168.88	247.5	168.88	INFINITY	106.8				
E-07	498725	254450	21	0.09	1.22	209.6	31.97	3.73	8.25	223.6	8.25	INFINITY	18.28				
E-08	498700	249875	6	0.02	0.64	950.9	2.83	19.59	2.83	18.53	66.88	18.53	INFINITY	13.91			
E-09	515300	281550	602	1.42	2.09	14.62	2.00	8.04	339.2	8.04	9.47	64.93	235.8	64.93	INFINITY	Low	
E-10	515520	280950	610	0.82	264.6	0.82	9.45	198.98	255.4	198.98	INFINITY	Low					
E-11	496050	253362.5	17	3.06	30.83	47.42	30.83	INFINITY	12.4								
E-12	499150	258325	34	2.68	18.57	96.21	18.57	INFINITY	29.6								
E-13	507650	285200	633	3.55	4.38	3.05	4.38	15.67	301.4	15.67	20.85	22.36	20.85	87.92	INFINITY	11.47	
E-14	508747.5	287250	775	0.24	8.68	84.52	8.68	84.52	210.5	40.8	INFINITY	8.94	8.94				
E-15	51762.5	285175	635	0.74	3.25	95.31	3.25	176.7	7.13	7.75	7.75	1.43	7.75	INFINITY	695.2		
E-16	511125	283912.5	641	0.03	5.56	57.49	5.56	10.89	209.2	10.89	15.51	1.92	15.51	41.71	INFINITY	Low	
E-17	509475	282975	495	1.52	8.15	947.2	8.15	99.05	147.1	99.05	INFINITY	Low					
E-18	495982.5	270850	232	1.33	9.50	85.89	9.50	11.53	10.25	11.53	18.09	High	18.09	47.34	INFINITY	520.4	
E-19	495287.5	268100	170	0.53	7.69	83.62	7.69	8.77	2.21	8.77	19.91	161.8	19.91	INFINITY	33.5		
E-20	499600	272700	287	0.77	8.19	66.07	8.19	14.41	162.9	14.41	95.28	35.43	95.28	INFINITY	351.3		
E-21	494975	257625	24	0.45	17.61	33.19	17.61	26.76	4.75	26.76	41.33	170.5	41.33	INFINITY	19.3		
E-22	495765	254700	16	3.09	5.12	143.1	5.12	23.64	37.77	23.64	INFINITY	14.82					
E-23	494925	250425	5	0.66	32.92	43.38	32.92	INFINITY	7.06								
E-24	509912.5	289650	772	1.27	1.6	4.05	1.6	13.37	30.45	13.37	39.59	81.78	39.59	42.01	INFINITY	1.71	
E-25	505687.5	286075	667	2.59	6.15	83.68	6.15	9.64	28.43	9.64	19.69	235.3	19.69	INFINITY	70.35		
E-26	502125	284487.5	645	0.92	5.01	185.5	5.01	9.23	70.88	9.23	53.28	215.5	53.28	INFINITY	55.43		
E-27	494375	270425	352	1.28	39.93	1.28	1.42	2.19	138.1	7.06	16.79	47.56	16.79	INFINITY	153.5		
E-28	498375	279462.5	381	1.66	8.28	31.82	8.28	15.29	300	15.29	20.97	4.68	20.97	INFINITY	144.8		
E-29	503537.5	282612.5	520	0	1.42	2005	1.42	17.52	220.5	17.52	INFINITY	50.49					
E-30	514180	279150	672	0.1	1.28	108.5	1.28	29.5	84.22	29.5	INFINITY	16.79					
E-31	505050	274662.5	505	2.53	6.44	170	6.44	11.73	6.02	11.73	55.94	205.1	55.94	72.46	INFINITY	Low	

LITHOLOGIC LOG

RESISTIVITY SOUNDING

SONDEO No. 30/89
 Cton. San Pablo
 SAN RAMON
 (ANDA - PLANSABAR)

E-01
 Coordinate-E: 508413m
 Coordinate-N: 285575m
 Elevation: 633m



ash: volcanic ash
 tf: tuff
 alv: andestic lava
 blv: basaltic lava
 wl: weathered layer
 s-g: sand and gravel
 ag: agglomerate
 agtf: tuff with agglomerate

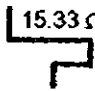
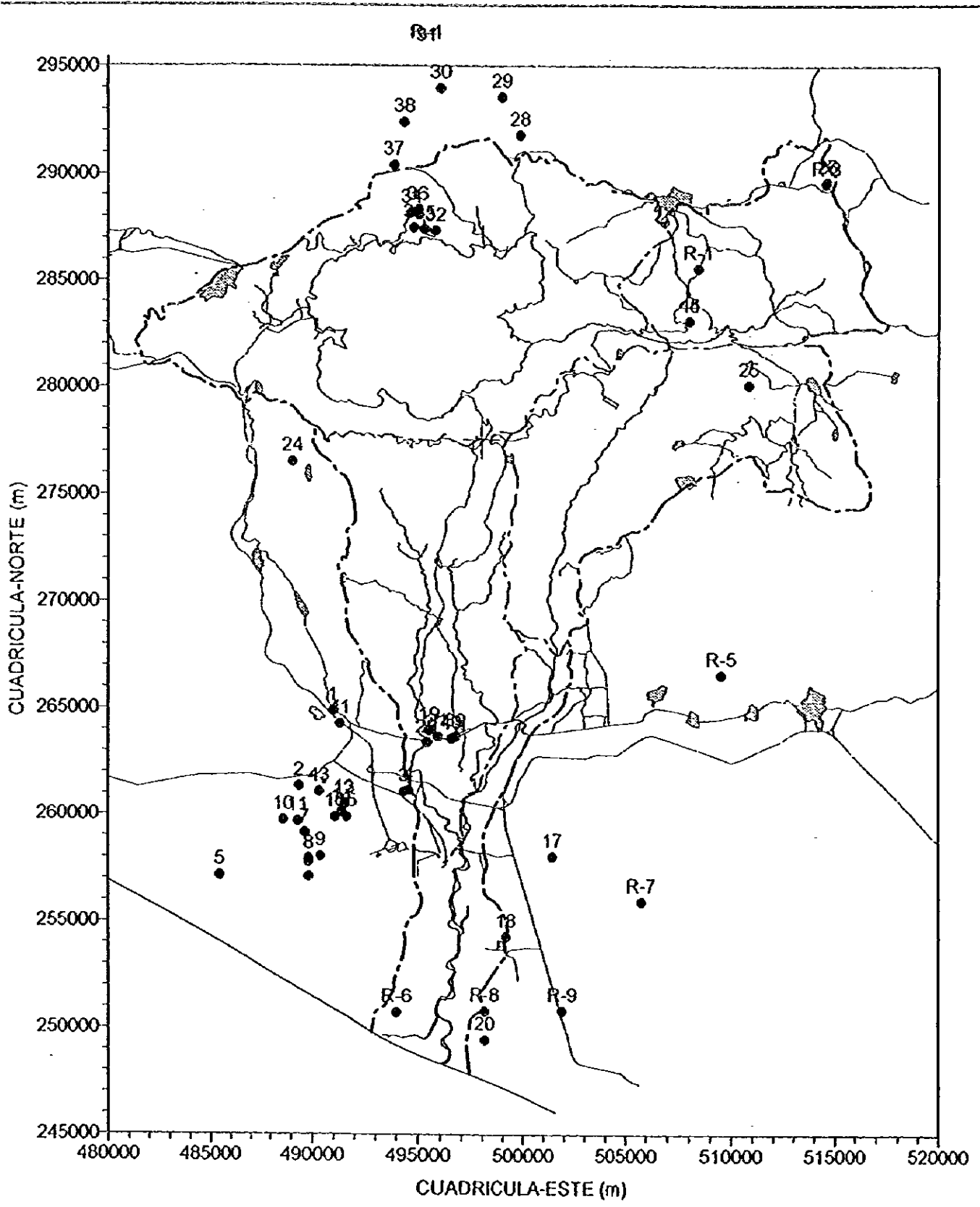
○ Field data (Apparent resistivity)
 15.33 Ω-m
 Inverse modelling result with resistivity

FIG.4 COMPARISON OF RESISTIVITY SOUNDING WITH LITHOLOGIC LOG AT E-01
 AGENCIA DE COOPERACION INTERNACIONAL DEL JAPON (JICA)

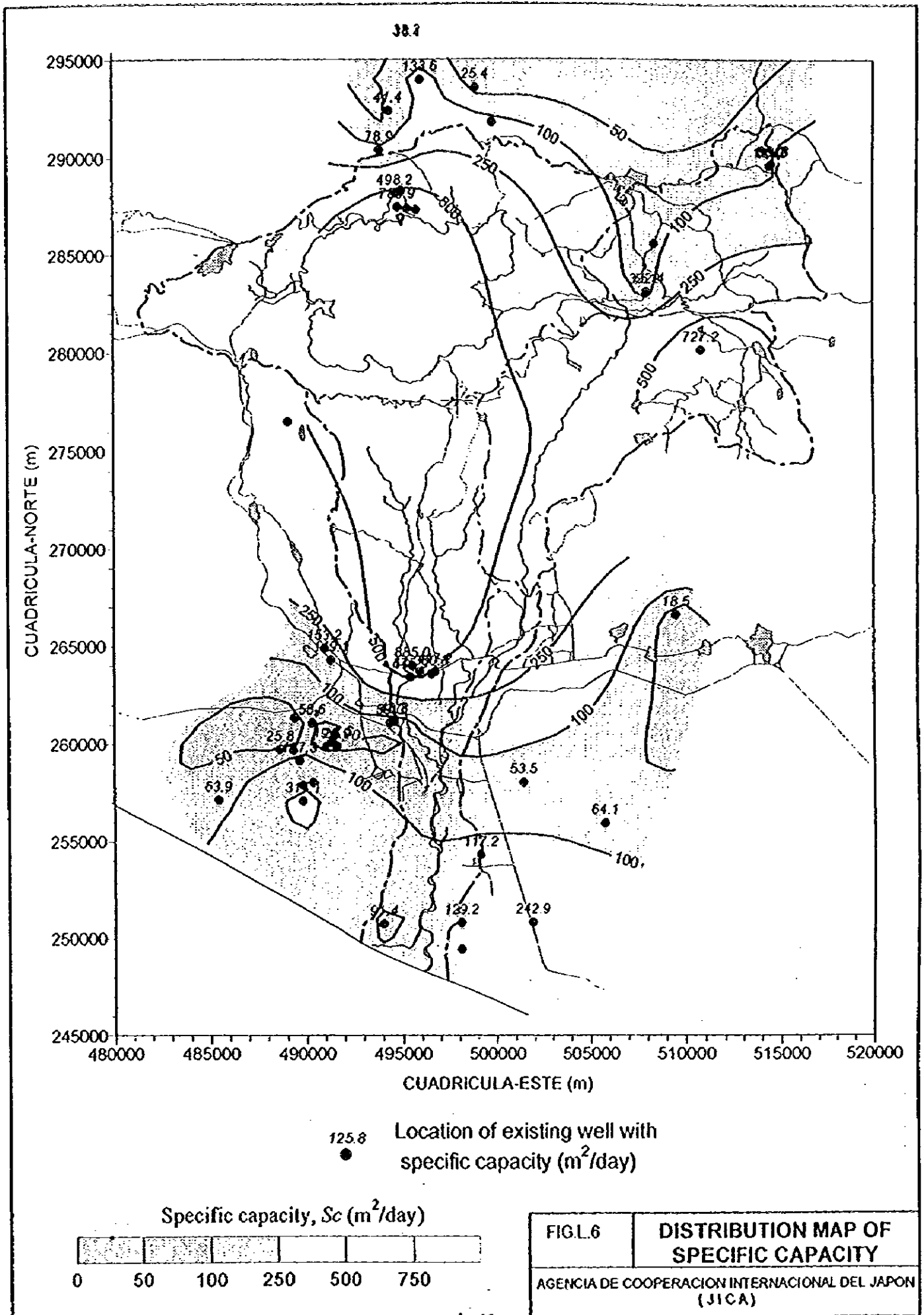
Table 4.1.3 LIST OF EXISTING WELLS RECORDS

Well No.	Original Well No.	CUADRICULA (m)		WELL DEPTH (m)	STATIC W.L. (m)	G.L. (m)	Discharge (lit)	Drawdown (m)	Sc (lit/m)	Sc (m ² /d)	T (m ² /d)	S	Pumping time (minute)
		NORTE	ESTE										
1	516	264300	490950	45.72	13.11	18.21	18.21	9.14	1.77	153.23	174		4320
2	660	261350	493350	65.94	11.36								1800
3	668	261100	494350	92.66	6.55								360
4	657	261150	494550	92.66	6.1								1000
5	656	257150	495400	79.55	1.83								1900
6	550	257100	496000	65.53	4.72								720
7	548	259150	496200	64.62	5.46								1390
8	546	257900	498800										
9	547	258050	490350										
10	546	259750	498600	60.90	4.45								
11	545	259700	499300										
12	544	260480	491470										
13	543	260550	491500										
14	542	260120	491350										
15	541	259900	491600	69.61	3.73								
16	540	259900	491050	71.02	4.57								
17	667	259050	501430	60.96	2.8								
18	663	264300	499150	31.4	6.61								
19	661	264000	498500	74.26	22.68								
20	659	269480	498100										
21	653	263700	495900										
22	652	263430	495410	91.44	18.29								
23	651	263430	495400	52.12	13.72								
24	517	276550	498050	105.68	9.14								
25	403	280100	510900	78	23.65								
26	358	285670	514570	103.63	11.58								
27	359	289670	514570	66.9	18.29								
28	372	291820	499825	90	40								
29	371	293600	499825	39.99	16.41								
30	370	294000	499000	116.67	55.75								
31	369	285750	495375	101.5	0.61								
32	714	287350	495775	165.63	460								
33	713	287500	494900	79.25	5.49								
34	712	286200	494675	58.4	11.5								
35	711	287425	495775										
36	710	288325	494975	158.5									
37	367	290425	493675	86.87	76.5								
38	366	292425	494350	112.78	39.83								
39	ROSARIO DE LA PAZ #1	263700	496700	52.10	18.28								
40	ROSARIO DE LA PAZ #2	263600	496500	85.32	18.28								
41	SAN JUAN TALPA	264300	491300	45.71	13.71								
42	POZO-2 SAN JUAN TALPA	261100	490300	73.13	20.57								
43	SAN LUIS	263100	508000	77.16	6.71								
44	CACAHUATL-2	263100	508000	31.36	0								
45	POZO-1 EL CACAHUATL	265575	509000	46.31	0								
R-1	Sn. Ramon	265575	509413	151.45	34.4								
R-2	Sn. Ramon Pozo-1	269575	514500	103.63	11.58								
R-3	Sn. Ramon Pozo-2	293050	495330	68.9	18.29								
R-4	Chalaban	266600	509575	110	63.56								
R-5	S7-10-89	250750	494000	33.9	-1.04								
R-6	S2-14-86	255950	506750	42	4.58								
R-7	S2-15-86	250825	496100	39.65	0.23								
R-8	S3-27-89	250850	501900	61.69	1.99								
R-9	S3-26-88	250850	501900	61.69	1.99								

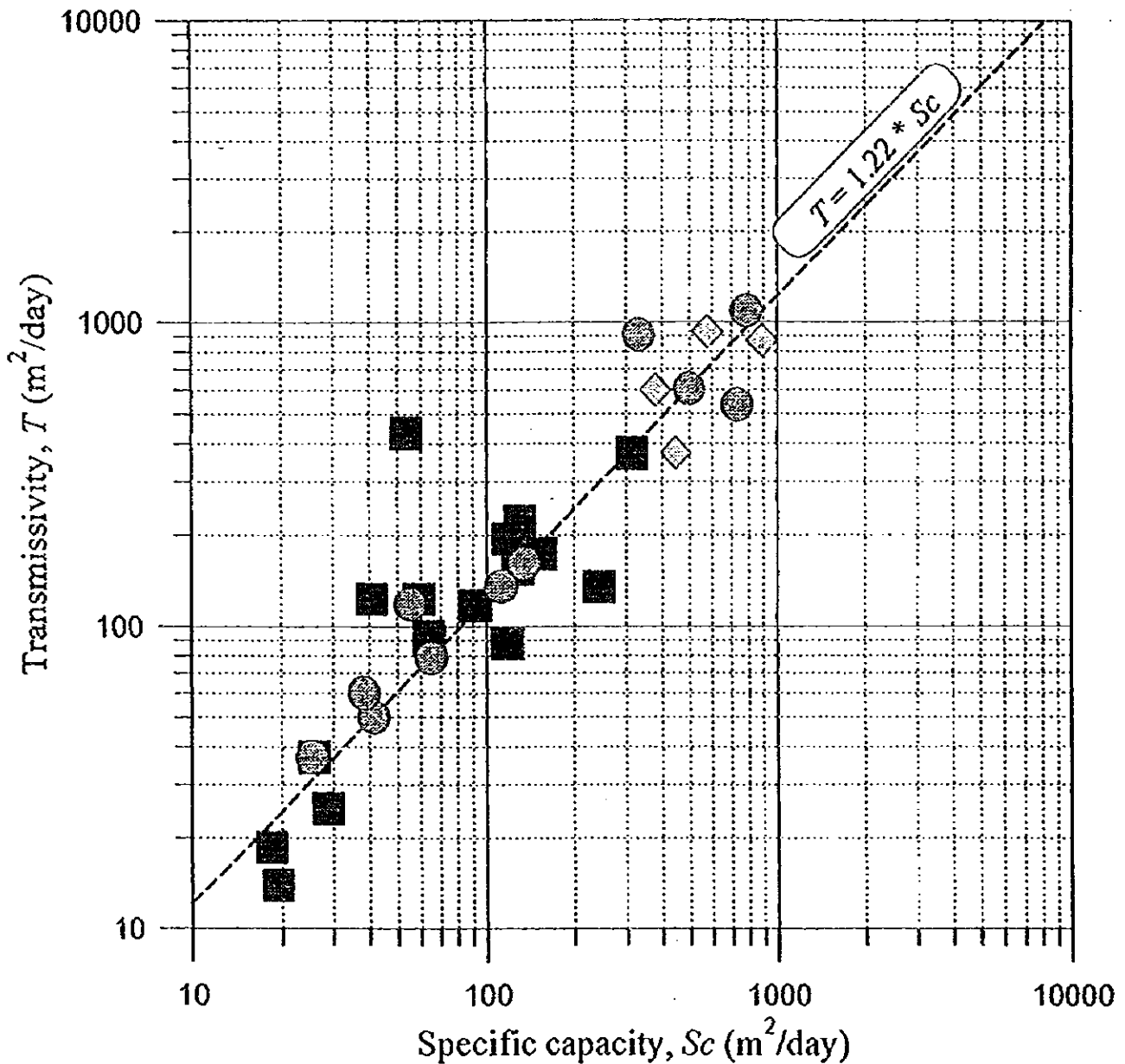


10 ● Location of existing well with No.

FIG.5	LOCATION OF EXISTING WELLS
AGENCIA DE COOPERACION INTERNACIONAL DEL JAPON (JICA)	

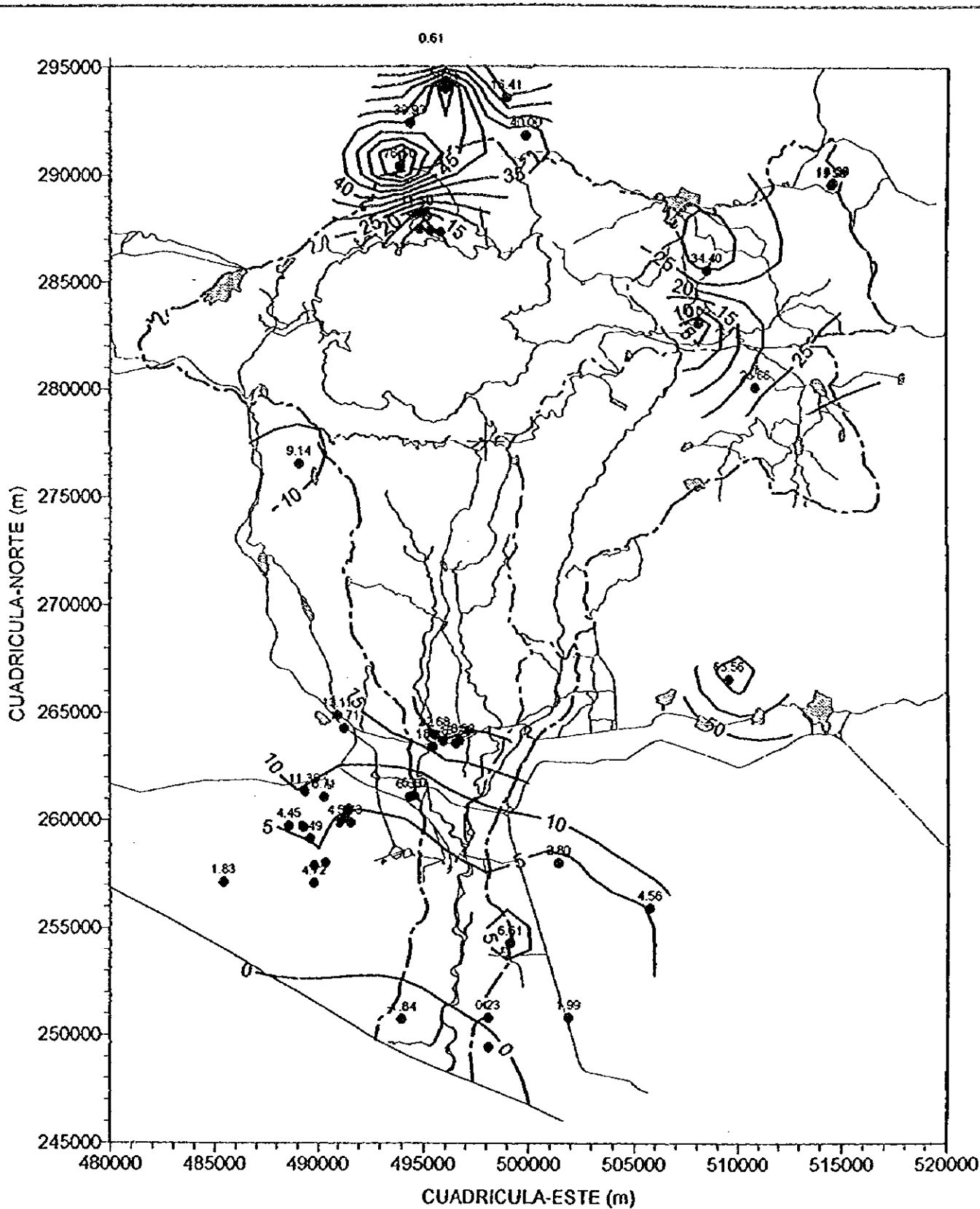


Relation between T and Sc



- Wells located in upstream area ($T = 1.234 Sc$)
- ◆ Wells located in El Rosario area ($T = 1.165 Sc$)
- Wells located in downstream area ($T = 1.189 Sc$)

FIG. 7	RELATION BETWEEN TRANSMISSIVITY AND SPECIFIC CAPACITY
AGENCIA DE COOPERACION INTERNACIONAL DEL JAPON (JICA)	



● 10.25 Location of existing well
 with depth to groundwater level
 from ground surface (in meter)

FIG.L.8	DEPTH TO GROUNDWATER LEVEL AT EXISTING WELLS
AGENCIA DE COOPERACION INTERNACIONAL DEL JAPON (JICA)	

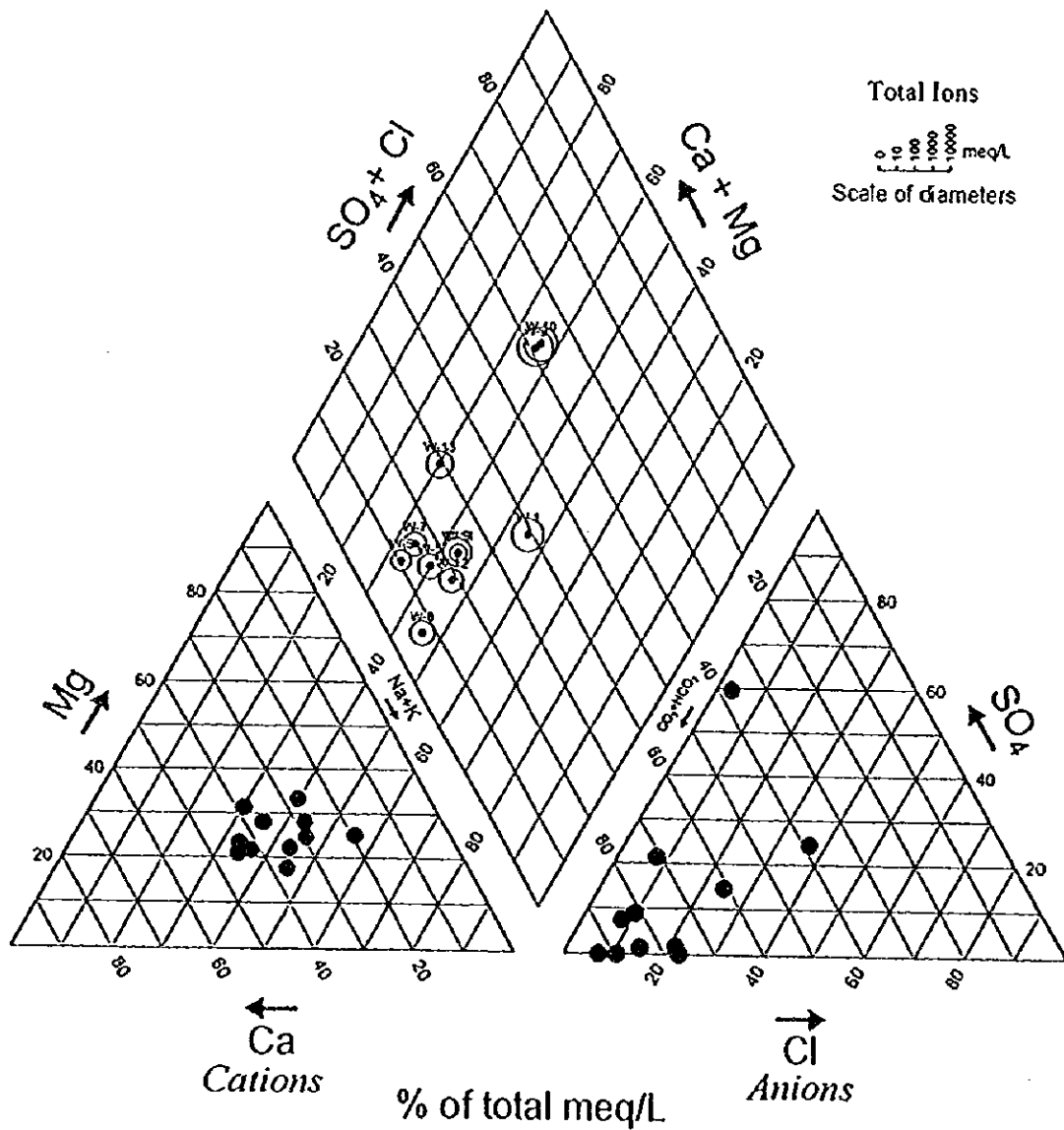


FIG. 9	TRILINEAR DIAGRAM OF GROUNDWATER (October 1996)
AGENCIA COOPERACION INTERNACIONAL DEL JAPON	

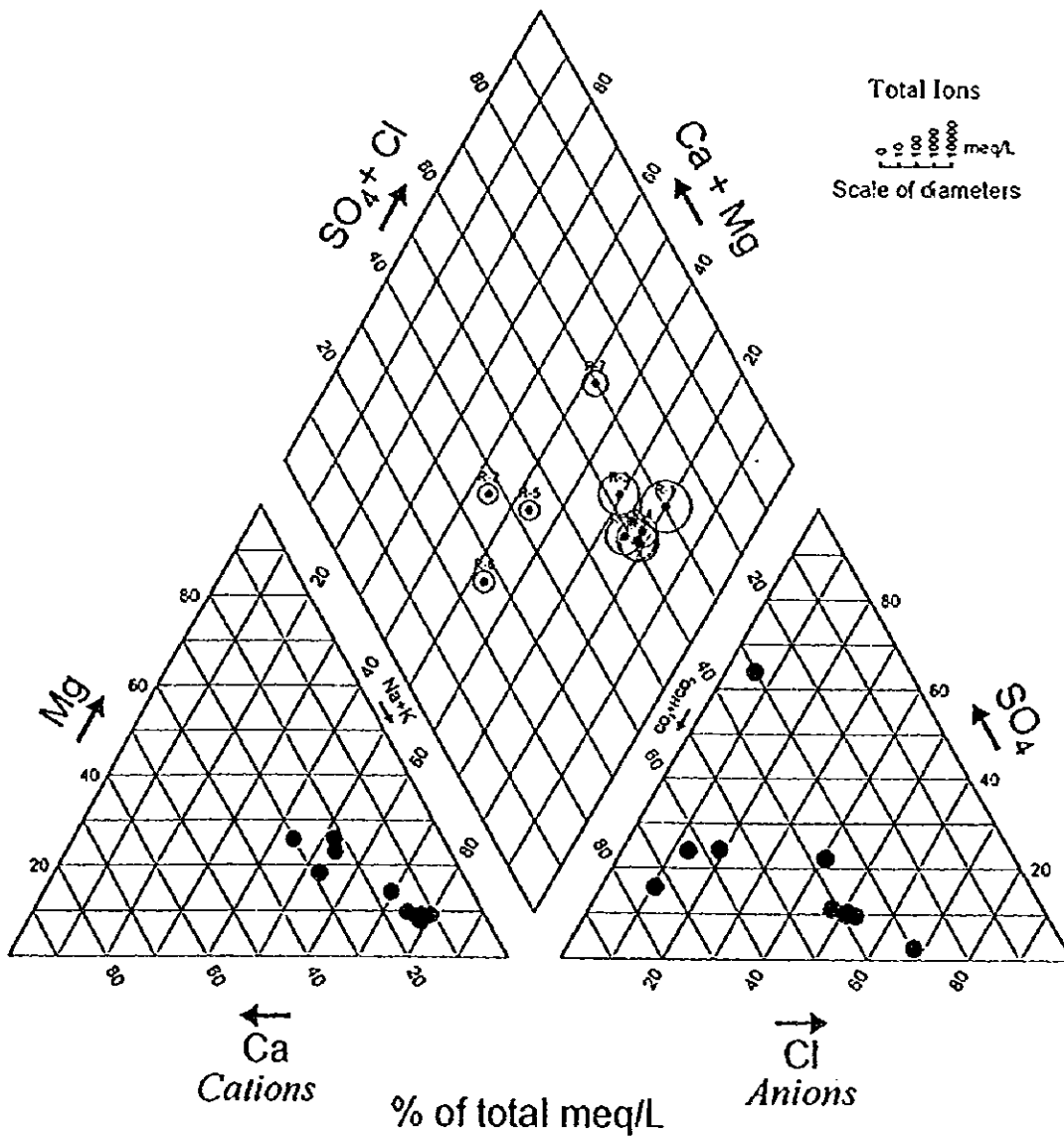


FIG.10	TRILINEAR DIAGRAM OF RIVER WATER (October 1996)
AGENCIA COOPERACION INTERNACIONAL DEL JAPON	

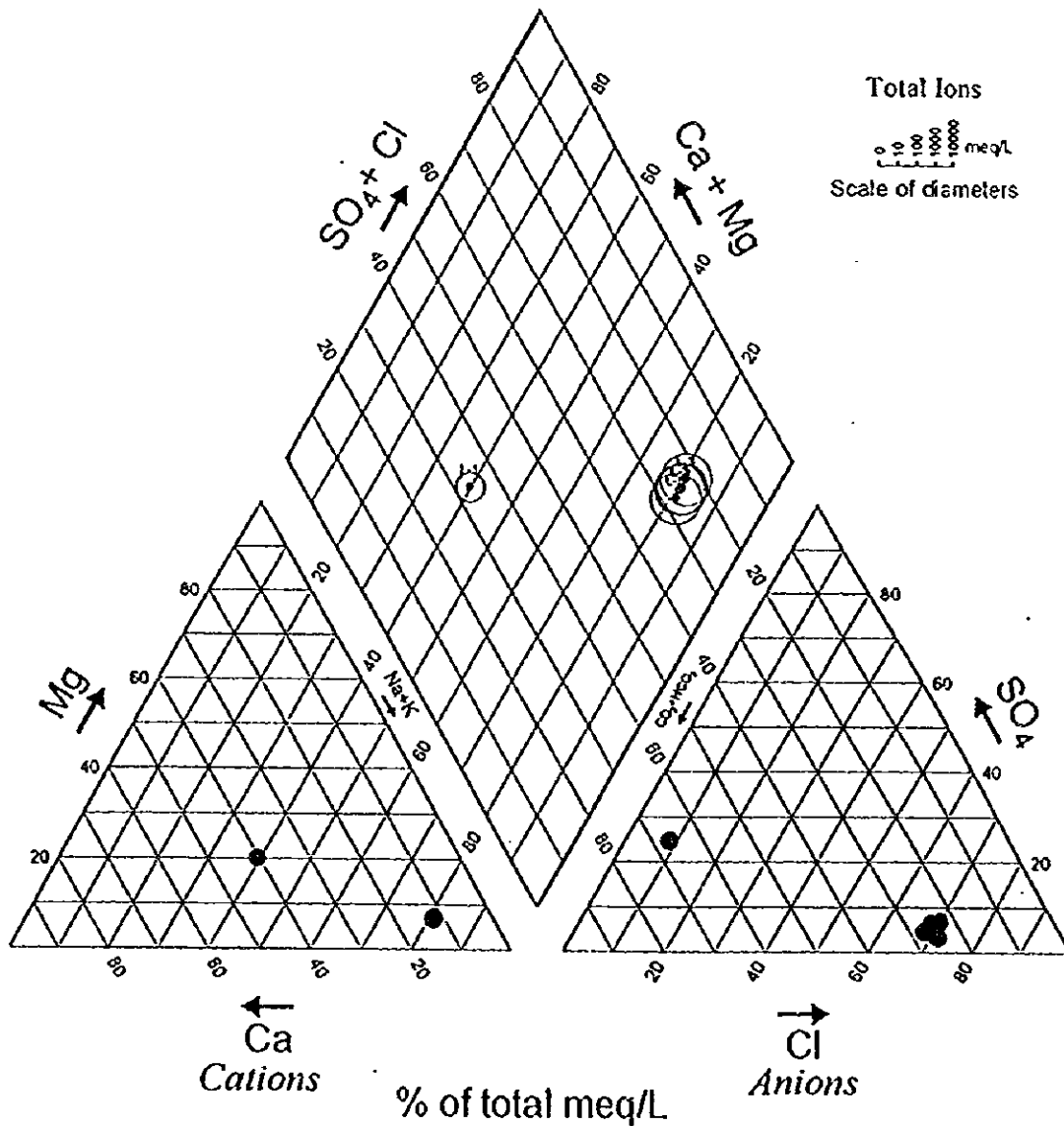
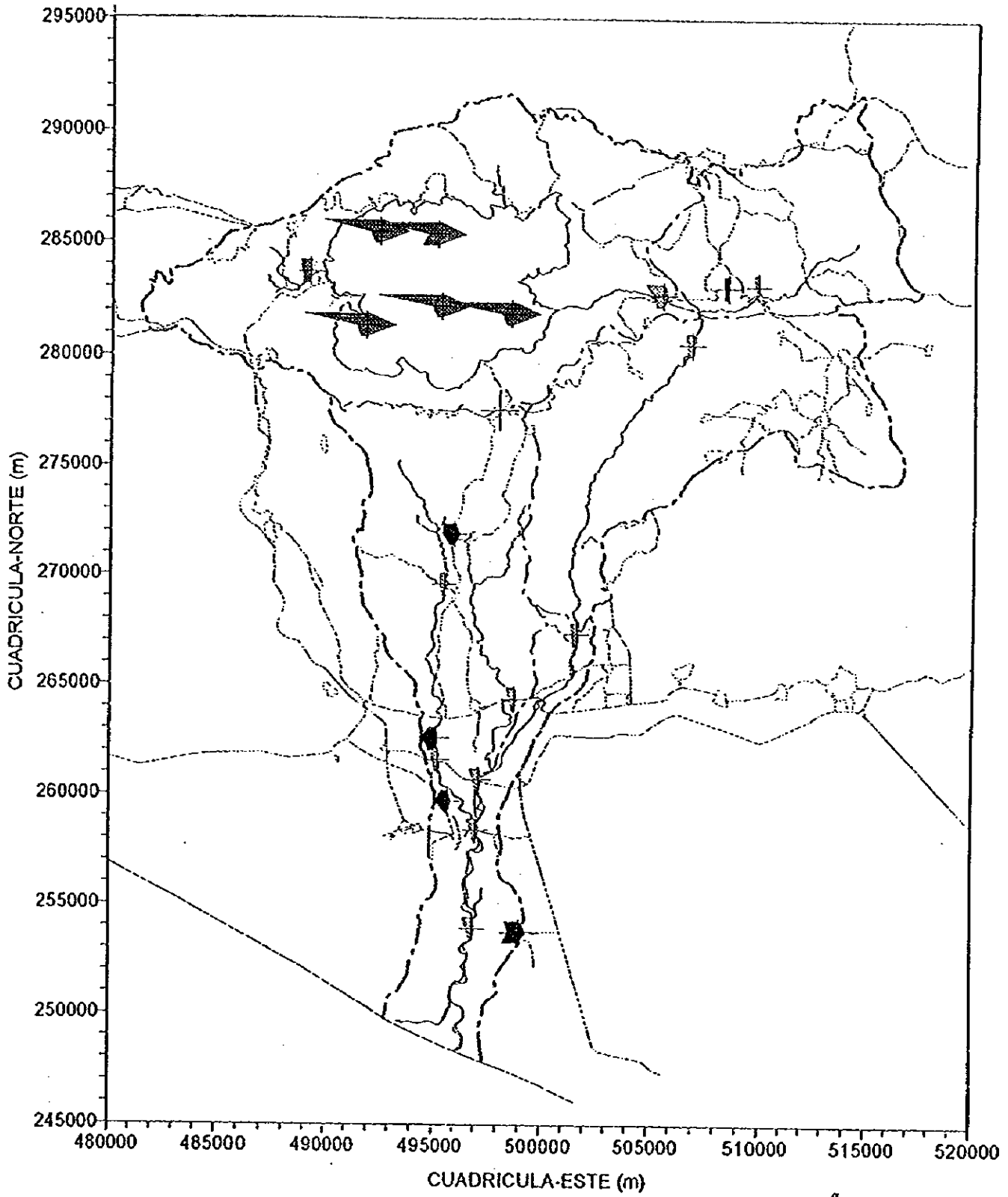





FIG. 11	TRILINEAR DIAGRAM OF ILOPANGO LAKE WATER (October 1996)
AGENCIA COOPERACION INTERNACIONAL DEL JAPON	



-  Lake water
-  River water
-  Groundwater

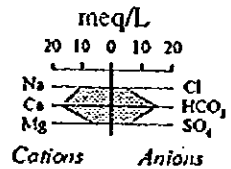
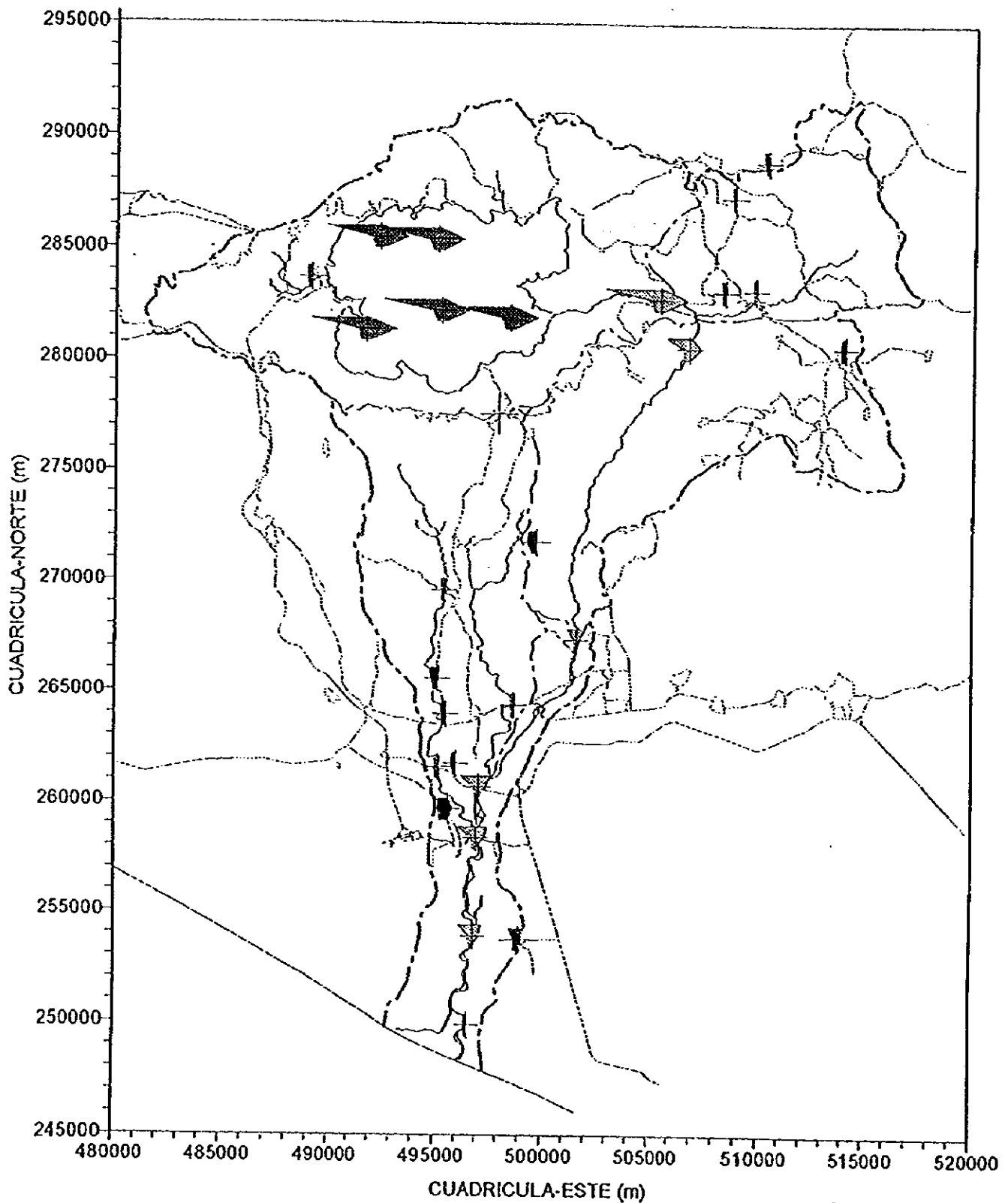



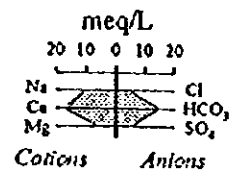


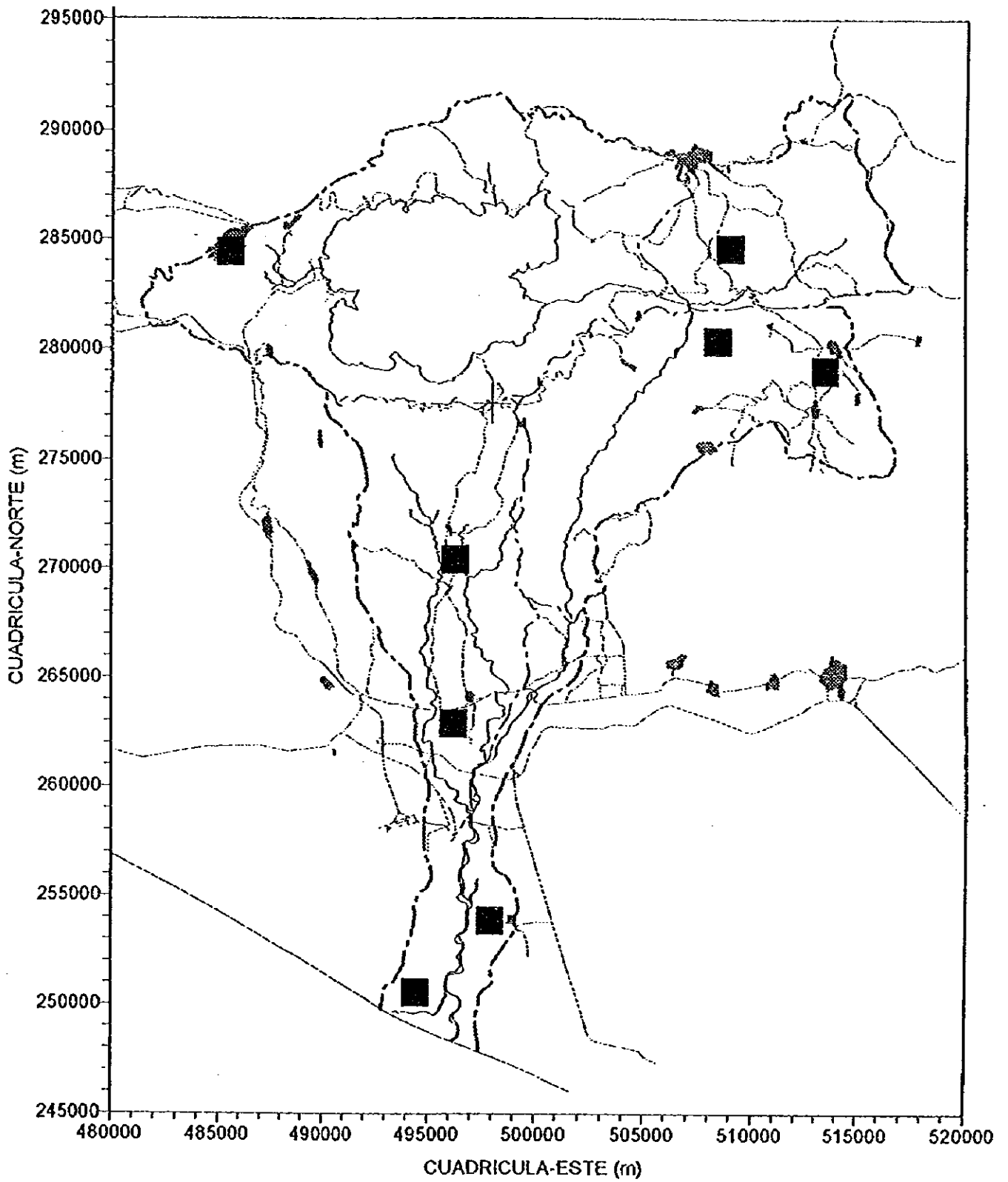
FIG.12 STIFF DIAGRAM OF WATER SAMPLES
(February 1996)
AGENCIA DE COOPERACION INTERNACIONAL DEL JAPON
(JICA)



-  Lake water
-  River water
-  Groundwater



FIGL 13	STIFF DIAGRAM OF WATER SAMPLES (October 1996)
AGENCIA DE COOPERACION INTERNACIONAL DEL JAPON (JICA)	



■ Location of proposed monitoring well

FIGL.14	PROPOSED LOCATIONS FOR GROUNDWATER MONITORING WELLS
AGENCIA DE COOPERACION INTERNACIONAL DEL JAPON (JICA)	

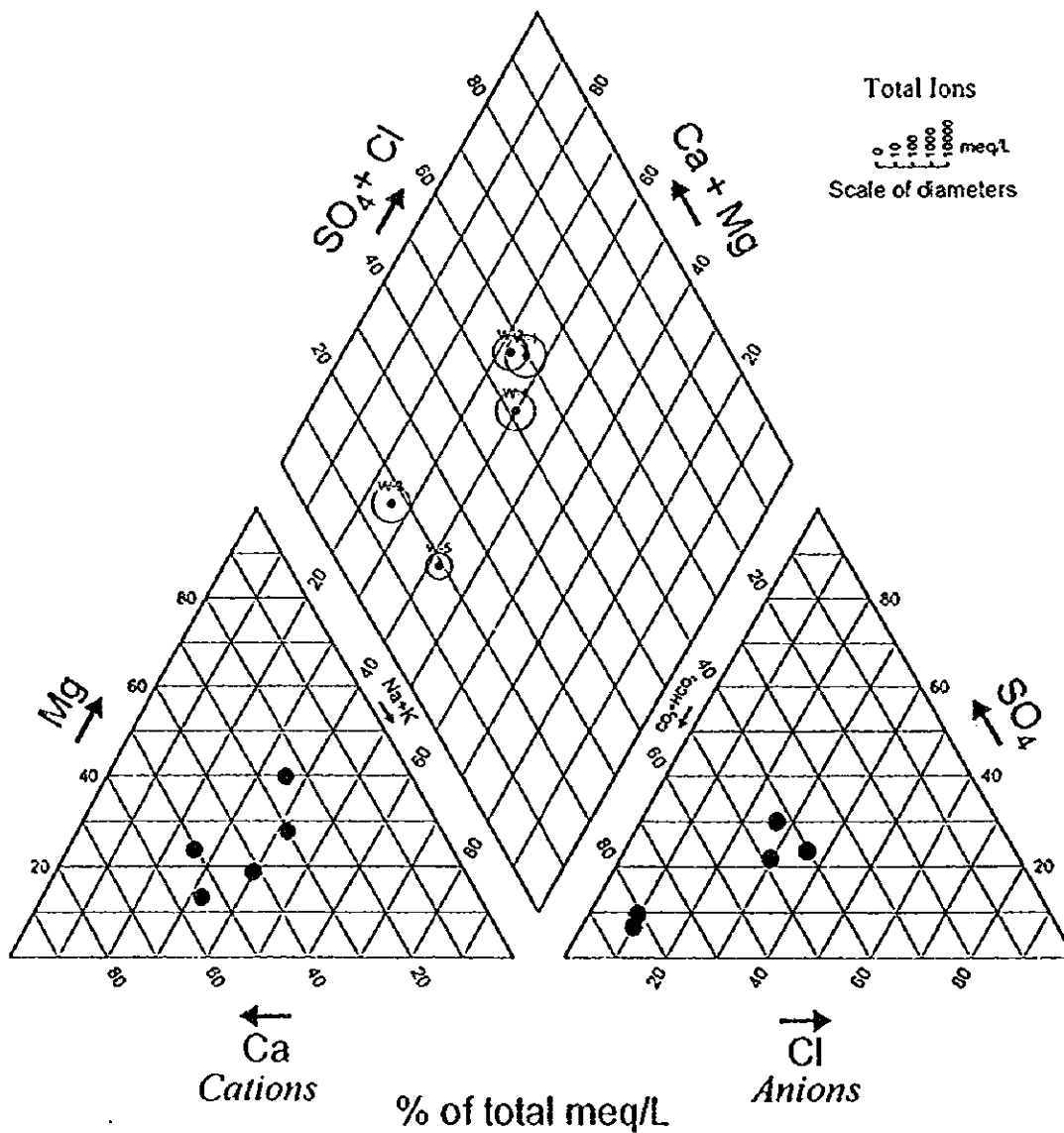


FIG.L.15

TRILINEAR DIAGRAM OF GROUNDWATER
(February 1996)

AGENCIA COOPERACION INTERNACIONAL DEL JAPON

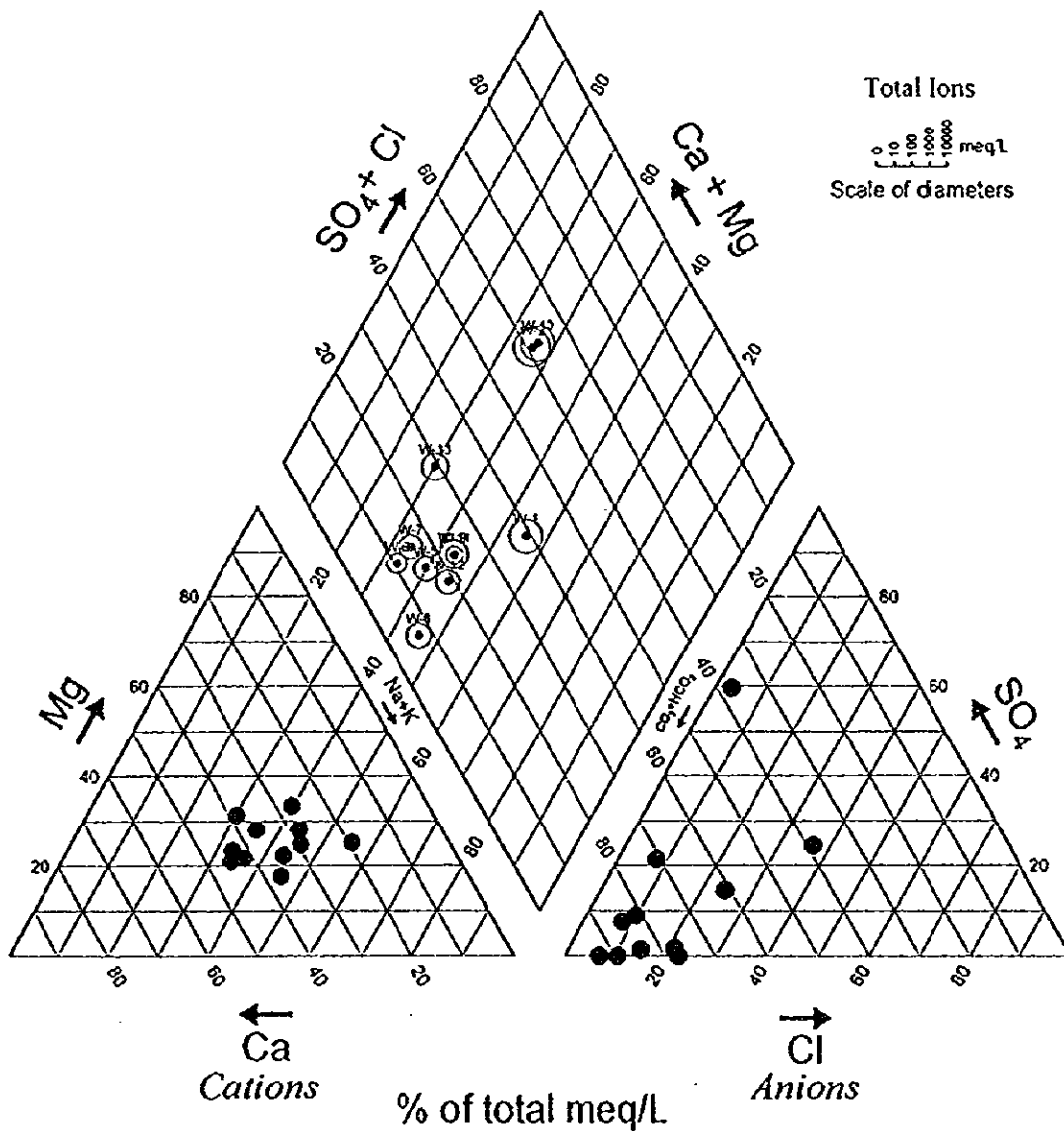


FIG.16	TRILINEAR DIAGRAM OF GROUNDWATER (October 1996)
AGENCIA COOPERATION INTERNACIONAL DEL JAPON	

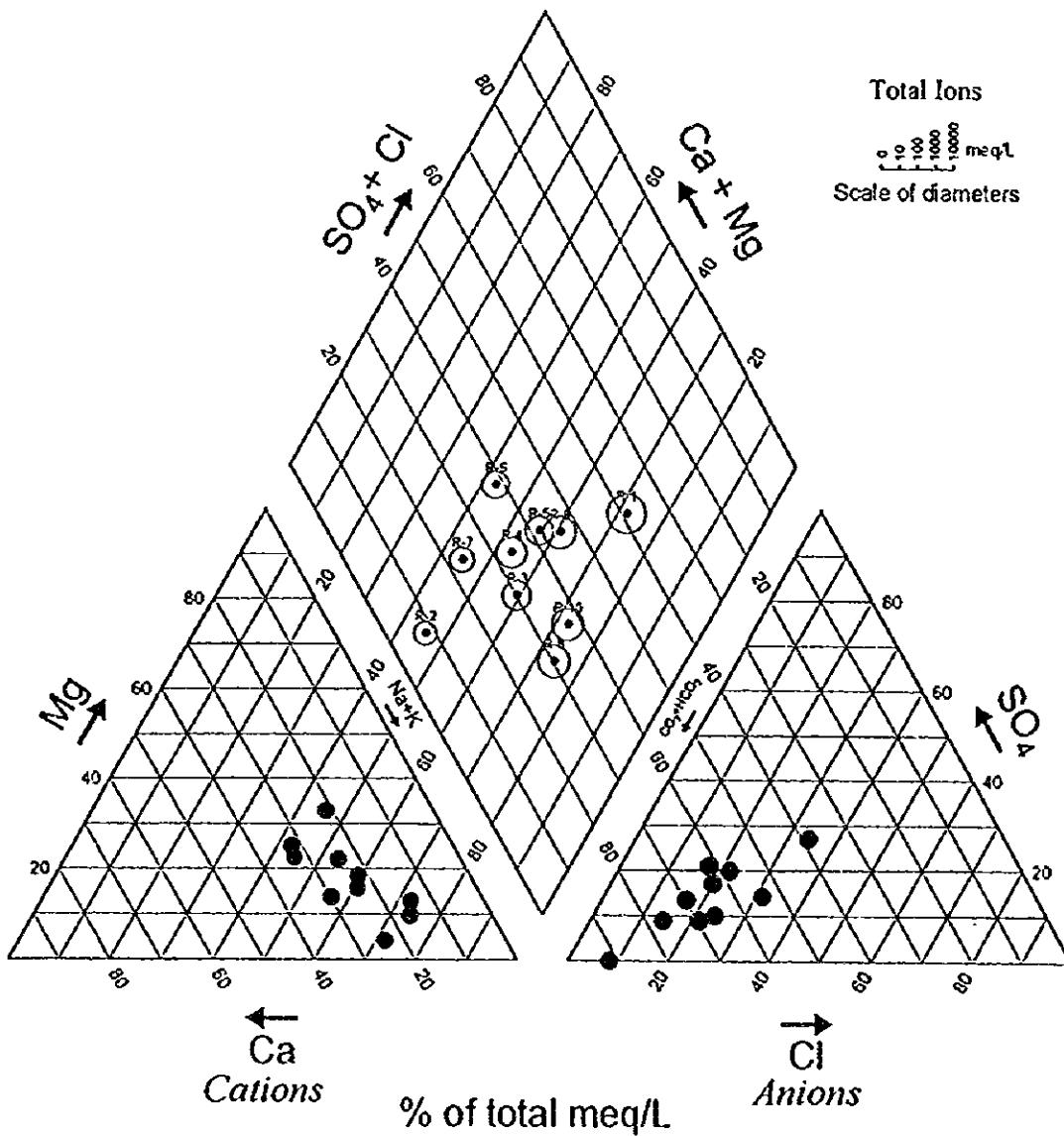


FIG.L17	TRILINEAR DIAGRAM OF RIVER WATER (Mid-February 1996)
AGENCIA COOPERACION INTERNACIONAL DEL JAPON	

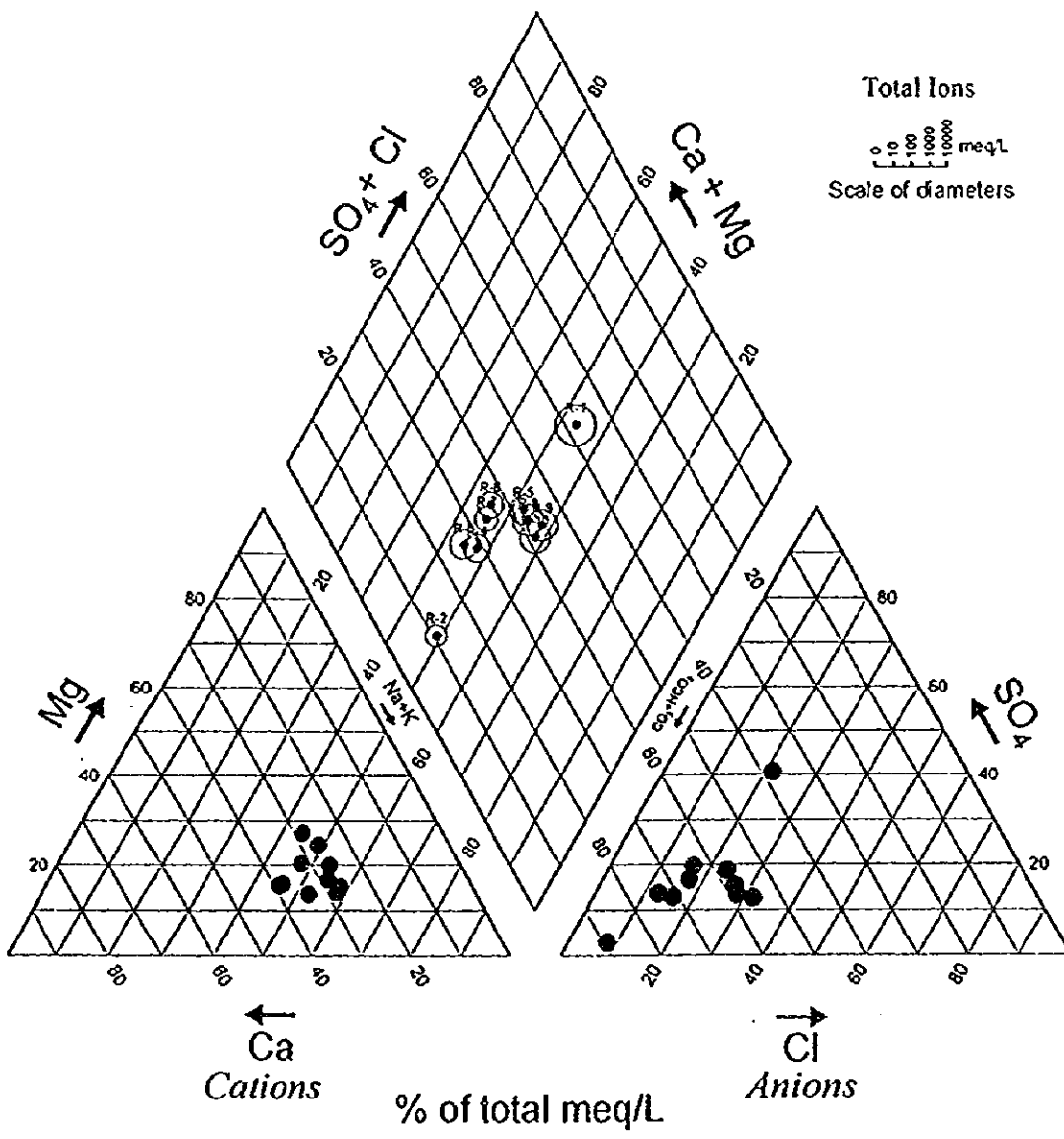


FIG.18	TRILINEAR DIAGRAM OF RIVER WATER (Late-February 1996)
AGENCIA COOPERACION INTERNACIONAL DEL JAPON	

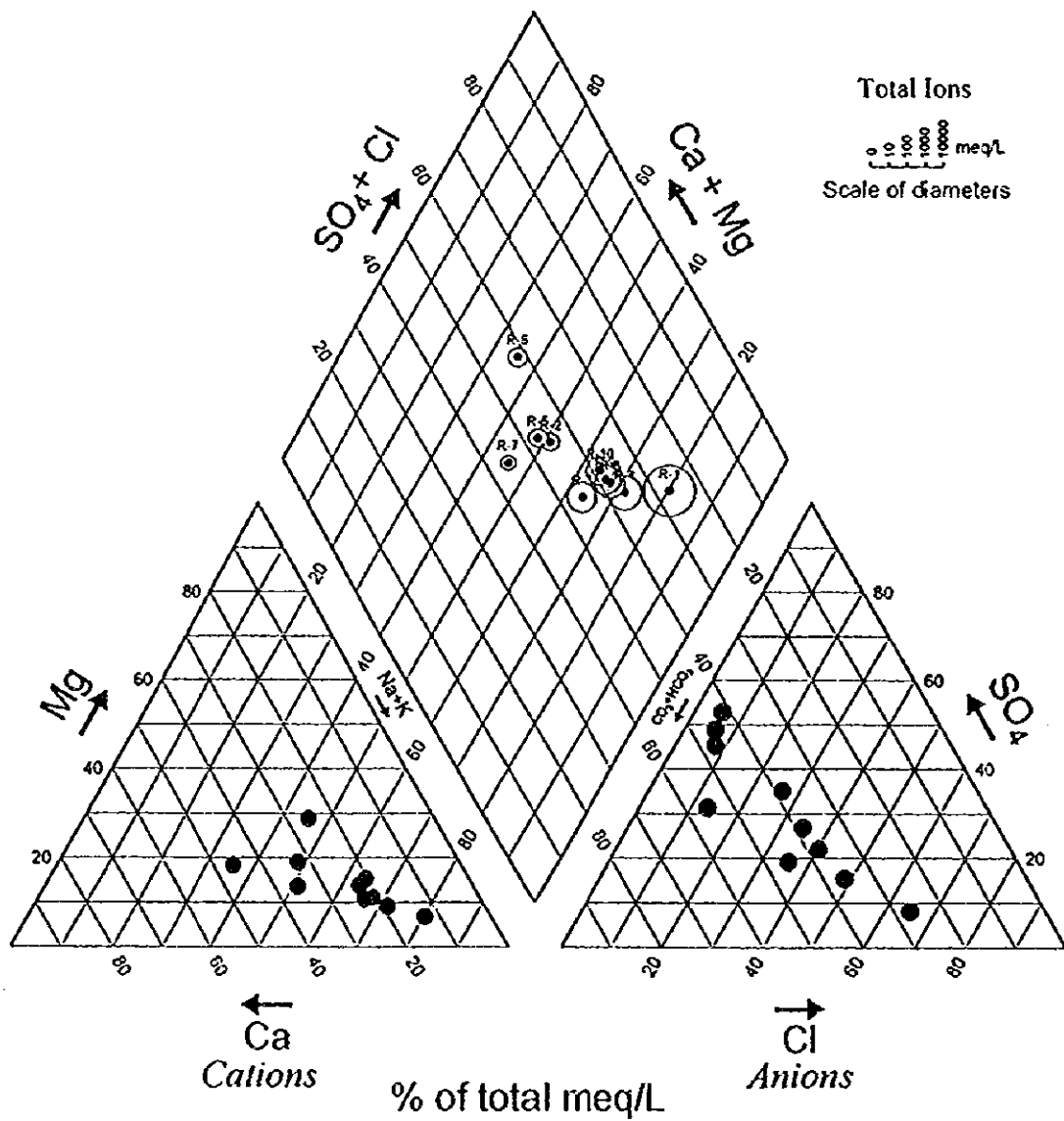
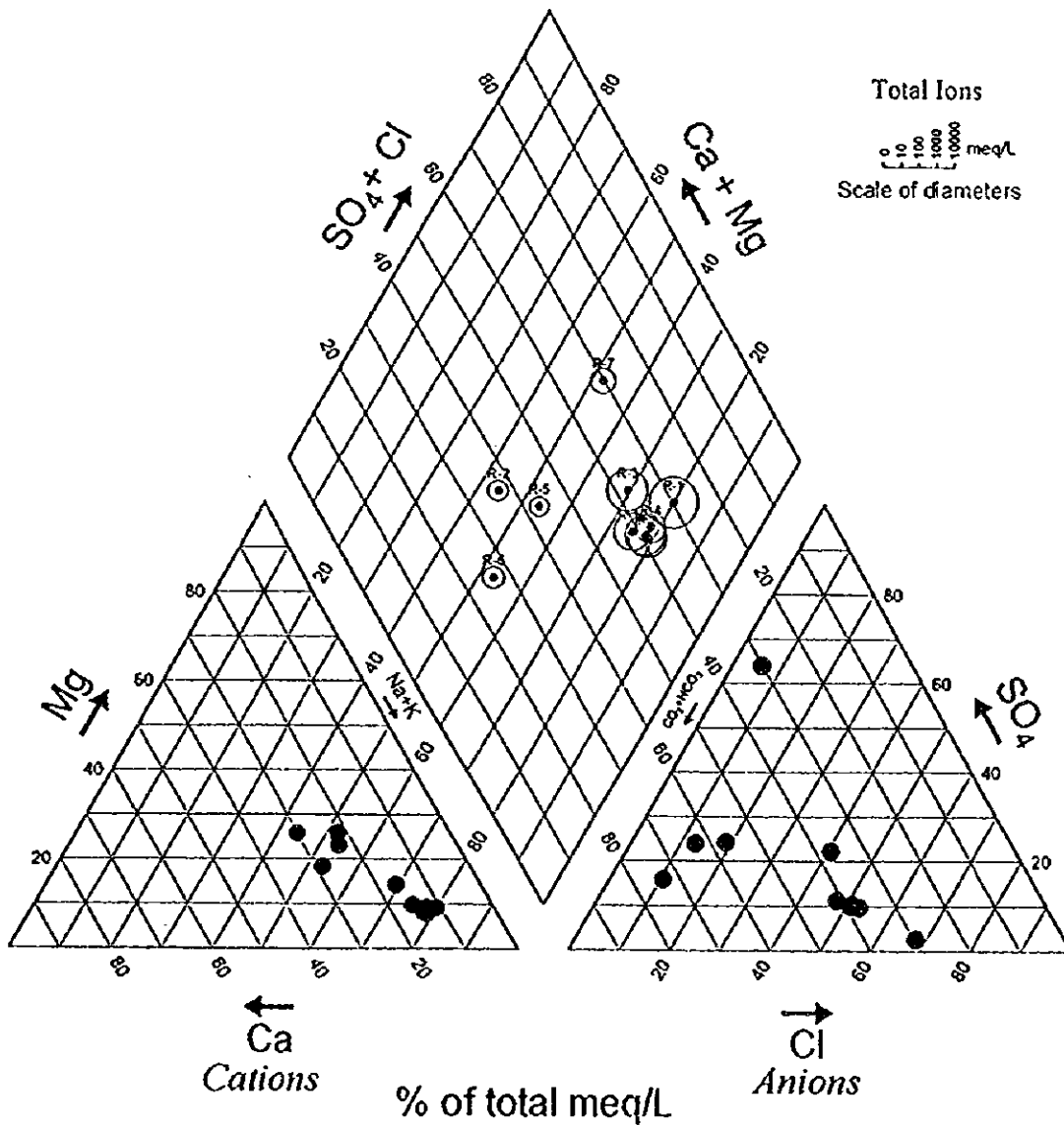


FIG.19	TRILINEAR DIAGRAM OF RIVER WATER (September 1996)
AGENCIA COOPERACION INTERNACIONAL DEL JAPON	



FIGL.20

TRILINEAR DIAGRAM OF RIVER WATER
(October 1996)

AGENCIA COOPERACION INTERNACIONAL DEL JAPON

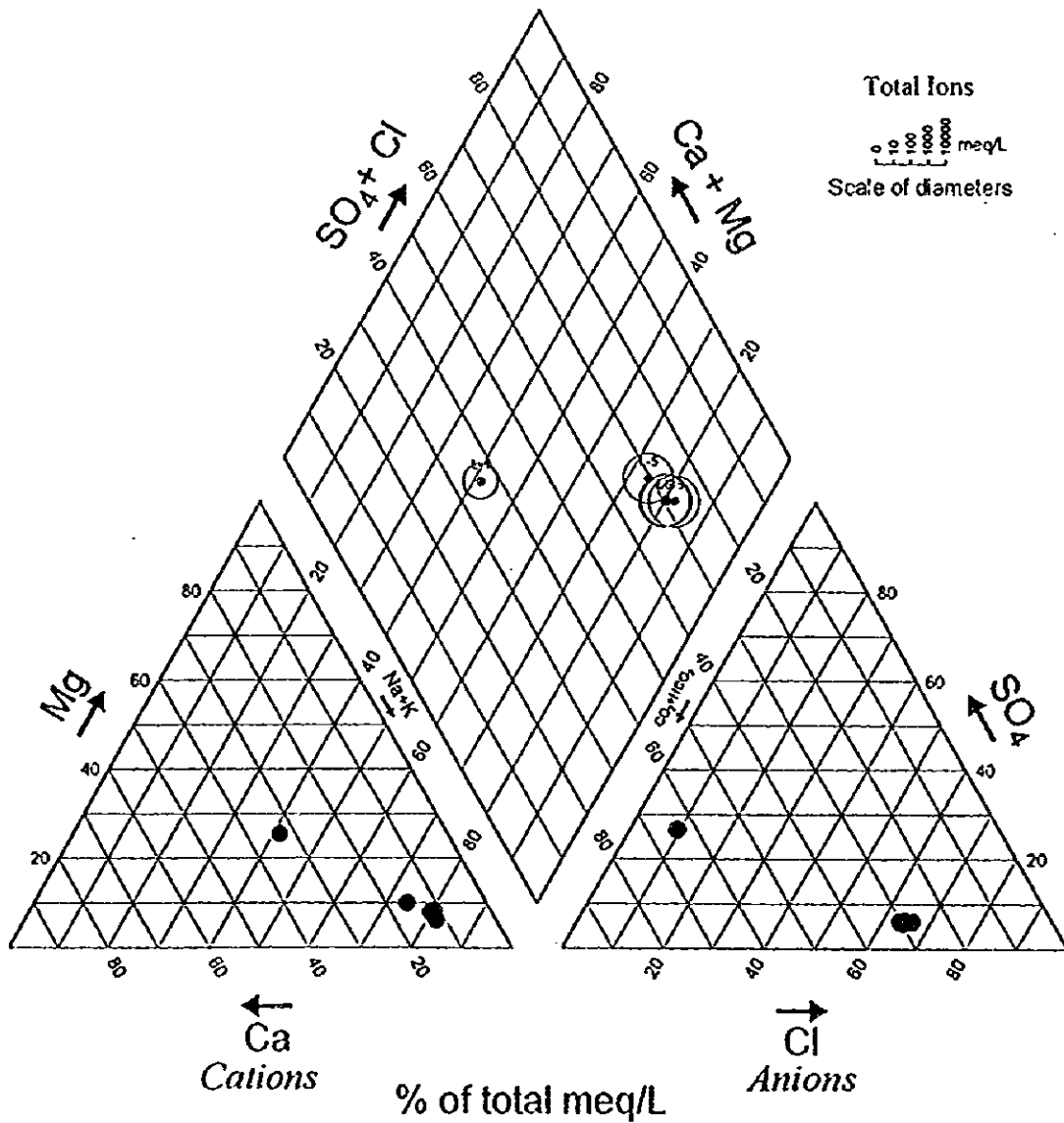


FIG.L.21	TRILINEAR DIAGRAM OF ILOPANGO LAKE WATER (Mid-February 1996)
AGENCIA COOPERACION INTERNACIONAL DEL JAPON	

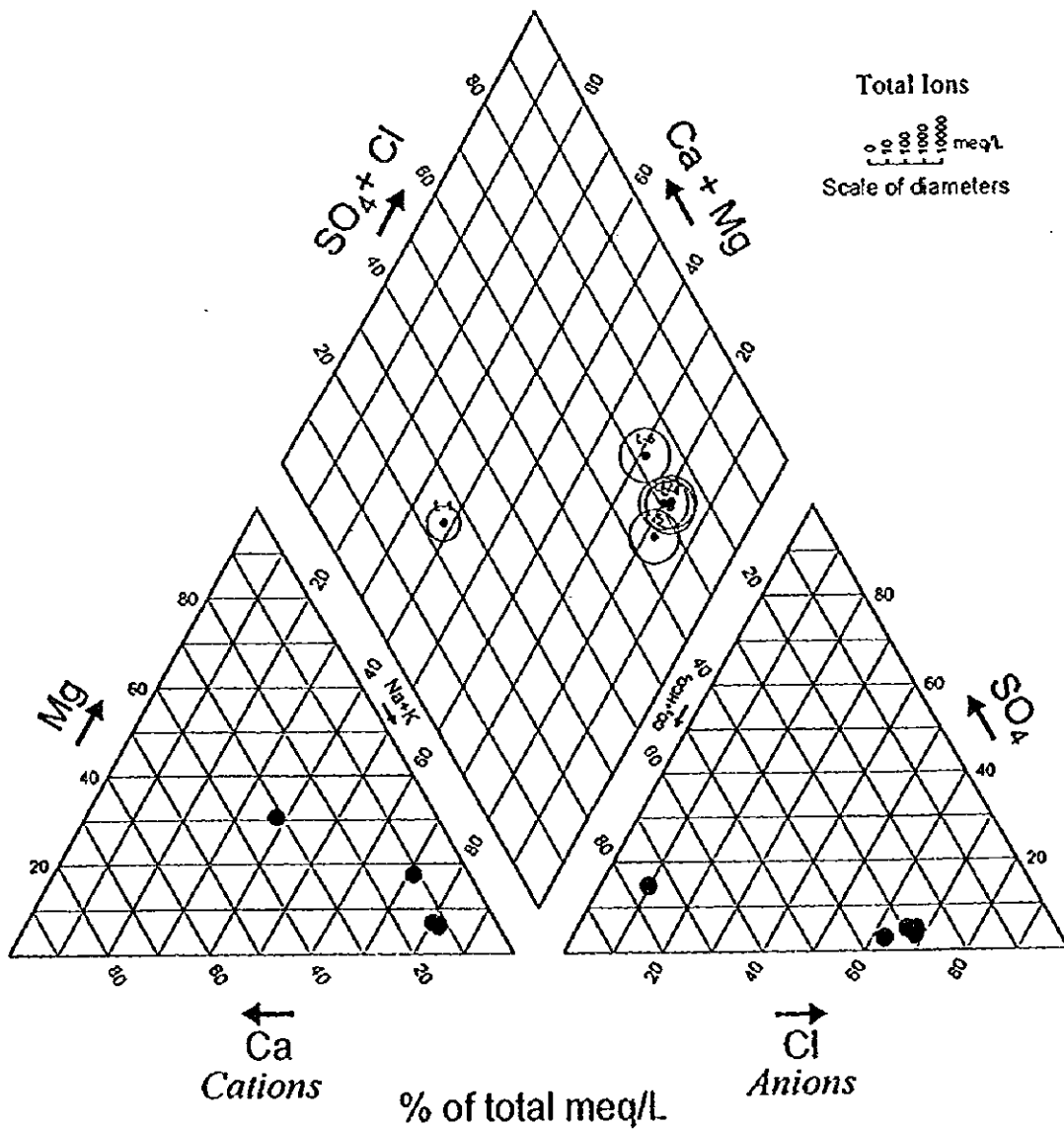


FIG.L.22	TRILINEAR DIAGRAM OF ILOPANGO LAKE WATER (Late-February 1996)
AGENCIA COOPERACION INTERNACIONAL DEL JAPON	

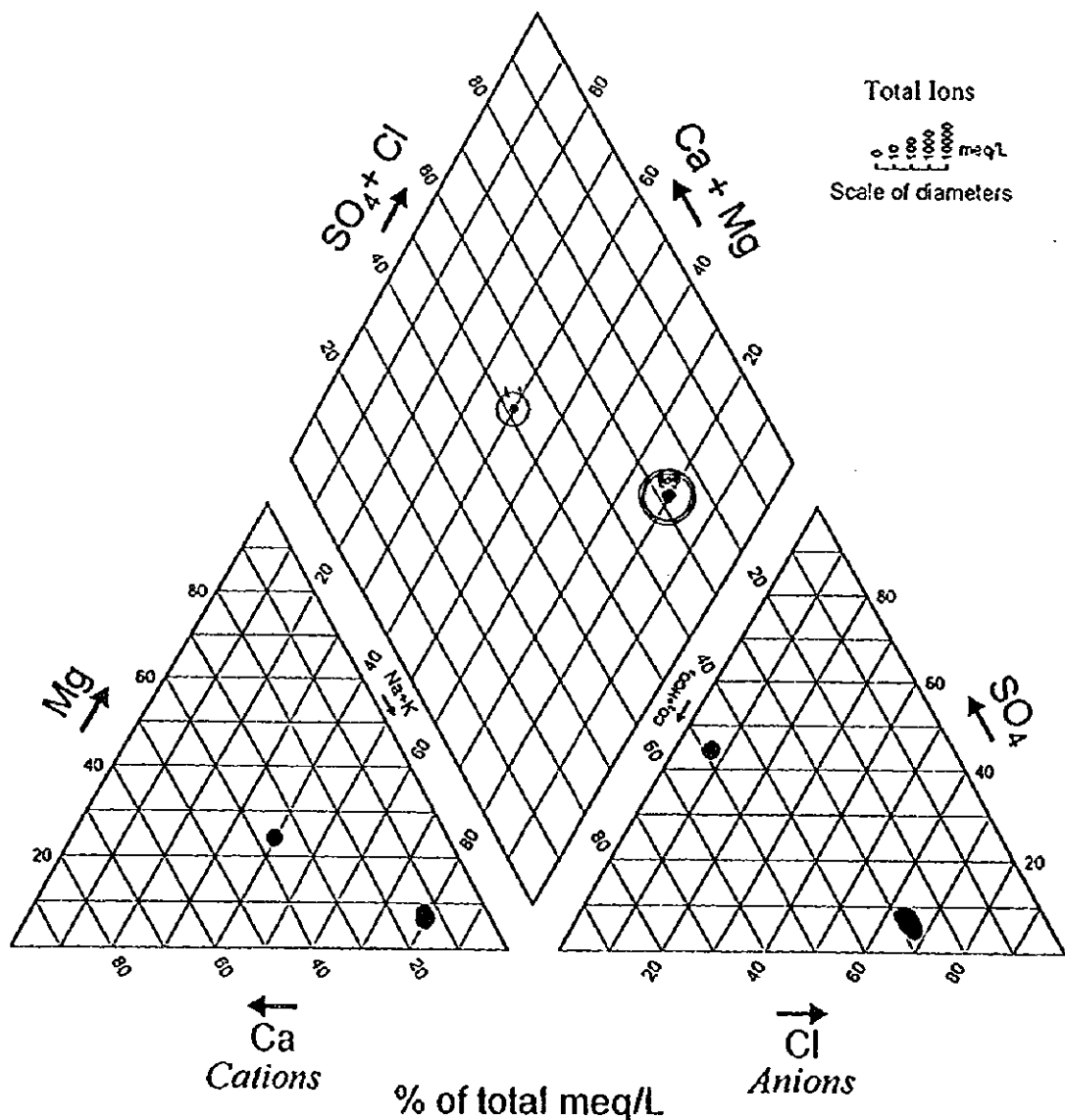


FIG. 23	TRILINEAR DIAGRAM OF ILOPANGO LAKE WATER (September 1996)
AGENCIA COOPERACION INTERNACIONAL DEL JAPON	

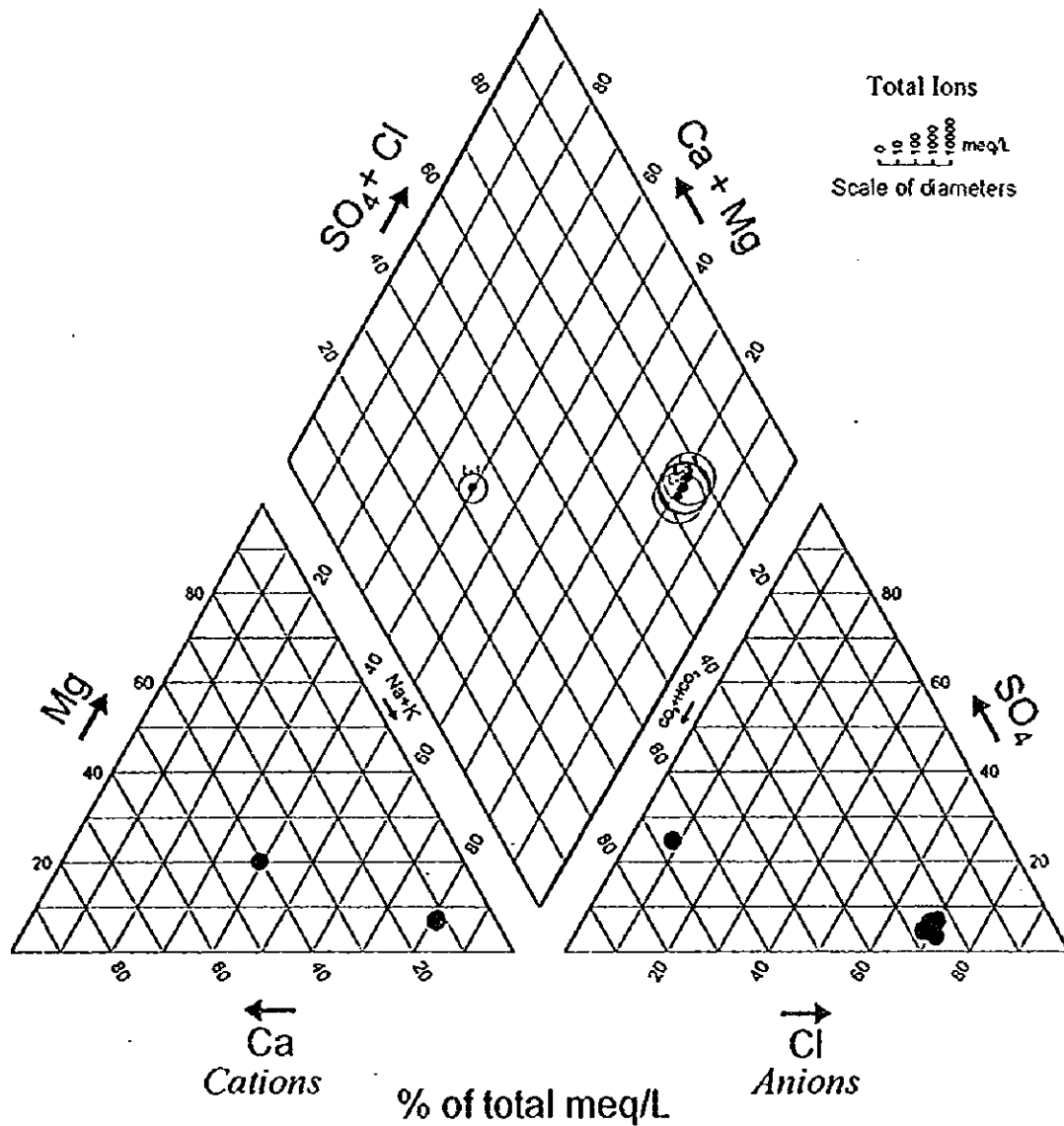


FIG.24	TRILINEAR DIAGRAM OF ILOPANGO LAKE WATER (October 1996)
AGENCIA COOPERACION INTERNACIONAL DEL JAPON	

